LOW-ENERGY ALINITE CEMENT PRODUCTION BY USING SODA WASTE SLUDGE

A THESIS SUBMITTED TO
THE GRADUATE SCHOOL OF NATURAL AND APPLIED SCIENCES
OF
MIDDLE EAST TECHNICAL UNIVERSITY

BY

GÜLTEKİN OZAN UÇAL

IN PARTIAL FULFILLMENT OF THE REQUIREMENTS
FOR
THE DEGREE OF MASTER OF SCIENCE
IN
CIVIL ENGINEERING

SEPTEMBER 2016

Approval of the thesis:

LOW-ENERGY ALINITE CEMENT PRODUCTION BY USING SODA WASTE SLUDGE

submitted by **GÜLTEKİN OZAN UÇAL** in partial fulfillment of the requirements for the degree of **Master of Science in Civil Engineering, Middle East Technical University** by,

Prof. Dr. Gülbin Dural Ünver _____
Dean, Graduate School of **Natural and Applied Sciences**

Prof. Dr. İsmail Özgür Yaman _____
Head of Department, **Civil Engineering**

Prof. Dr. Mustafa Tokyay _____
Supervisor, **Civil Engineering Dept., METU**

Examining Committee Members:

Prof. Dr. Kambiz Ramyar _____
Civil Eng. Dept., Ege University

Prof. Dr. Mustafa Tokyay _____
Civil Eng. Dept., METU

Prof. Dr. İsmail Özgür Yaman _____
Civil Eng. Dept., METU

Assoc. Prof. Dr. Sinan Turhan Erdoğan _____
Civil Eng. Dept., METU

Assoc. Prof. Dr. Mustafa Şahmaran _____
Civil Eng. Dept., Gazi University

Date: 06.09.2016

I hereby declare that all information in this document has been obtained and presented in accordance with academic rules and ethical conduct. I also declare that, as required by these rules and conduct, I have fully cited and referenced all material and results that are not original to this work.

Name, Last name: Gültekin Ozan Uçal

Signature:

ABSTRACT

LOW-ENERGY ALINITE CEMENT PRODUCTION BY USING SODA WASTE SLUDGE

Uçal, Gültekin Ozan
M.S., Department of Civil Engineering
Supervisor: Prof. Dr. Mustafa TOKYAY

September 2016, 61 pages

Increased environmental awareness and the concept of sustainable development have impacts on cement industry as on many other fields. Alinite cement which was developed in the 1970s may be an alternative inorganic, low energy binding material. In this study, synthesis and optimization of the properties of alinite cement was carried out by using soda waste sludge as a raw material.

Soda waste sludge was mixed with limestone, clay, and iron ore in different proportions. All mixes were burned at 1050^{o}C or 1150^{o}C to produce alinite cement clinker. 1, 2, and 4 hours of calcination times were applied and the clinkers were examined by chemical and mineralogical analysis. Optimal burning temperature and calcination time were determined. Chemical analyses were carried out by X-Ray Fluorescence spectroscopy and by wet chemical analysis. Mineralogical analyses were performed by X-Ray Diffraction (XRD) technique.

Based on chemical and mineralogical analyses, suitable clinkers were selected and produced in larger quantities. They were ground and mixed with gypsum. Effects of gypsum content on compressive strength and calorimetry values were investigated and compared to a commercially available portland cement. Mineral

phases present in the course of hydration were determined by powder XRD. Observation of crystal structures at different hydration ages was also carried out, by scanning electron microscopy (SEM).

It was shown that soda waste sludge can be used to produce low-energy and low-CO_2 alinite cement with sufficient properties. Compressive strengths comparable to ordinary portland cement can be achieved with partial replacement of limestone with soda waste sludge in the raw mix. Short setting time of alinite cement associated with fast initial rate of reaction was also noted.

Keywords: Alinite cement, low-energy cement, soda waste sludge

ÖZ

SODA ATIK ÇAMURUNDAN

DÜŞÜK ENERJİLİ ALİNİT ÇİMENTOSU ÜRETİMİ

Uçal, Gültekin Ozan
Yüksek Lisans, İnşaat Mühendisliği Bölümü
Tez Yöneticisi: Prof. Dr. Mustafa TOKYAY

Eylül 2016, 61 sayfa

Artan çevre bilinci ve sürdürülebilir kalkınma kavramı pek çok endüstri gibi çimento endüstrisini de etkilemektedir. 1970'lerde geliştirilen alinit çimentosu düşük enerjili ve inorganik alternatif bir bağlayıcı malzeme olma potansiyeline sahiptir. Bu çalışmada soda atık çamuru kullanılarak alinit çimentosu sentezi ve çimento özelliklerinin optimizasyonu üzerine çalışılmıştır.

Soda atık çamuru farklı oranlarda kalker, kil ve demir cevheri ile karıştırılmıştır. Alinite çimentosu üretmek için bütün karışımlar 1050^{o}C ve 1150^{o}C yanma sıcaklığında pişirilmiştir. Yanma süresi olarak 1, 2 ve 4 saat uygulanmış olup elde edilen klinkerler kimyasal ve mineralojik analize tabi tutulmuş, böylece en uygun yanma sıcaklığı ve yanma süresi belirlenmiştir. Kimyasal analizler X-Işınları Floresans spektroskopisi yöntemi ve kimyasal yaş analizle, mineralojik analizler X-Işınları Difraktometri yöntemi ile yapılmıştır.

Kimyasal ve mineralojik analiz sonuçlarına dayanarak uygun bulunan klinkerler seçilmiş ve öğütülüp alçı taşı ile karıştırmak için daha büyük miktarlarda üretilmiştir. Alçı taşı katkısı oranının basınç dayanımı ve kalorimetre sonuçlarına olan etkisi araştırılmış ve sonuçlar piyasada satılan bir portland çimentosuyla mukayese edilmiştir. Hidratasyon süresince ortaya çıkan ürünler toz X-Ray difraksiyonu yöntemiyle belirlenmiştir. Ayrıca, farklı yaşlardaki numunelerde bulunan kristal yapılar taramalı elektron mikroskobu ile görüntülenmiştir.

Araştırmalar sonucunda soda atık çamurunun yeterli özelliğe sahip düşük enerjili ve düşük CO_2 değerli alinit çimentosu üretiminde kullanılabileceği gösterilmiştir. Kuru karışımdaki kalkerin soda atık çamuruyla kısmi ikamesi sonucunda normal portland çimentosuyla kıyaslanabilir basınç dayanımı sonuçları elde edilmiştir. Alinit çimentosunun yüksek erken reaksiyon hızına bağlı olarak hızlı priz aldığı kaydedilmiştir.

Anahtar Kelimeler: Alinit çimentosu, düşük enerjili çimento, soda atık çamuru

ACKNOWLEDGEMENTS

I would like to express my sincere gratitude to Dr. Mustafa Tokyay. His guidance and support throughout this study was more than helpful. I consider myself fortunate to have a supervisor with whom anyone would wish to work.

My great thanks to Dr. İsmail Özgür Yaman and Dr. Sinan Turhan Erdoğan, for all their contributions regarding this thesis and my master's study.

Special thanks to my fellow researcher Mahdi Mahyar, who was with me during experiments. His lab experience made each step easier.

The treatment I got from Materials of Construction Laboratory crew was much appreciated. Day after day, I greeted them with questions and received nothing but kind answers.

Greetings to my fellow research assistants, who shared all the joyous times of writing a thesis with me.

I am grateful to my fiancée, whose understanding knows no boundaries when it comes to my study.

I thank Votorantim Çimento A.Ş. Hasanoğlan Cement Plant for providing us raw materials and bags of portland cement necessary in this research.

I thank Şişecam Soda Sanayii A.Ş Mersin Soda Plant for providing us their soda waste.

Finally, I would like to thank The Scientific and Technological Research Council of Turkey (TÜBİTAK) for making this extensive research possible by providing funding.

TABLE OF CONTENTS

LIST OF TABLES

TABLES

LIST OF FIGURES

FIGURES

LIST OF ABBREVIATIONS

d : Day

EDX : Energy-Dispersive X-Ray Spectroscopy

h : Hour

ICP-OES : Inductively Coupled Plasma Optical Emission Spectrometry

kN : Kilonewton

LI : Lime Index

LOI : Loss on Ignition

LSF : Lime Saturation Factor

LSF_{mod} : Chlorine Modified Lime Saturation Factor

min : Minute

MPa : Megapascal (N/mm^2)

PC : Portland Cement

s : Second

SEM : Scanning Electron Microscope

SWS : Soda Waste Sludge

wt% : Weight Percentage

w/c : Water/Cement Ratio

XRD : X-Ray Diffraction

XRF : X-Ray Fluorescence

CHAPTER 1

INTRODUCTION

1.1 General

The world is in an age of rapid construction. Due to its versatility, relatively higher durability, abundance, and relative cheapness, concrete has been a primary material of construction for a long time. More than 4 billion tons of cement, which is the main binder in concrete, is produced worldwide annually (van Oss, 2015). Steady consumption in developed countries, huge infrastructure and superstructure investments necessary in developing countries and the potential of underdeveloped regions ensure this level of demand in the future, if not grow any further.

Cement production, however, is an energy intensive process. On average, around 4.2 GJ of energy is consumed per 1 ton of portland cement clinker production, and even in modern rotary kilns, approximately 870 kg of CO_2 is released to the atmosphere during the process (Tokyay, 2016). This is the reason why cement industry is responsible for 5% of global human-made carbon dioxide emissions (Hendriks et al., 2002).

Considering the situation above, radical changes are needed to be adapted in production and development techniques. Institutions and scientists try to find new ways of minimizing negative impact on environment caused by human activity, and alinite cement is one such effort in cement industry.

1.2 Objectives and Scope

The aim of this thesis is to determine the applicability of soda waste sludge in producing cementitious materials. Soda waste sludge primarily consists of $CaCO_3$, $Ca(OH)_2$, and $CaCl_2$ in an aqueous solution. The high chlorine content of soda waste sludge is the major drawback for its use as an admixture or additive in cementitious systems since chlorine is strictly limited by standards due to durability concerns. Therefore, using this waste, production potential of alinite cement was investigated, which contains bound chloride within its hydration products.

To produce alinite cement, soda waste sludge was used along with traditional clinker raw materials; limestone, clay, and iron ore. Since chlorine content in soda waste sludge is too high, it is used as partial replacement of limestone in two of the raw mixes. Chemical and mineralogical analyses of clinkers with different sludge contents, different maximum burning temperatures and different calcination periods (duration of burning at maximum temperature) were compared using XRF and XRD techniques.

Based on these experimental investigations, promising mixes were interground with different amounts of gypsum to observe changes in physical and mechanical properties. Energy requirements during grinding were also observed. CEM I 42.5R type portland cement (abbreviated in the thesis as PC) was obtained from Votorantim cement plant to compare hydration characteristics of alinite cement to that of commercially available portland cements.

Chapter 2 includes background and literature review about sustainability, the concept of low energy cements, alinite as a cementitious phase, alinite cement as a hydraulic binder, and soda waste sludge of Solvay process.

Chapter 3 includes raw mix proportioning and details of experimental procedures.

Chapter 4 displays and discusses the experimental results.

Chapter 5 includes conclusions and summary of the study along with future recommendations.

CHAPTER 2

BACKGROUND AND LITERATURE REVIEW

2.1 Sustainability

Human progress is at a point where development without considering its side effects is no longer viable. By the end of 21st century, global mean temperature is expected to rise 1.1-6.4 ^{o}C, mainly because of accumulation of greenhouse gases that are increasingly emitted to the atmosphere due to human activity (IPCC, 2007). A comprehensive shift from living at the expense of nature to living with nature is necessary for continuation of a habitable earth.

Local availability and relative cheapness ensure portland cement's role in construction industry in predictable future, however, search for more economical alternatives and regulations regarding environmental concerns will increasingly pressure cement industry to seek sustainable solutions. Being responsible as one of the major causes of carbon dioxide emissions throughout the world, cement industry has disadvantages and advantages regarding this issue.

On the downside, harmful emission of cement industry is enormous. It requires serious reductions. Yet, one of the principle reactions in the production of portland cement clinker, main ingredient of most commercially available cements, is the calcination. That is, dissociation of carbon dioxide from calcium carbonate, which is mostly in the form of limestone and chalk, to use remaining calcium oxide in the clinkering process.

Reaction: $CaCO_3 \rightarrow CaO + CO_2$ (1)

Molar weights in g: $100 \rightarrow 56 + 44$ (2)

As calcium oxide constitutes around two thirds of portland cement clinker, approximately 500 kg of carbon dioxide is released to the atmosphere per ton of portland cement clinker produced, due to calcination alone. When emissions resulted from fuel for heating and grinding operations, and production of consumed electricity are included, this value goes up considerably.

On the other hand, it is an encouraging fact that wide range of materials, including some wastes, can be successfully utilized within cementitious systems. Fly ash from thermal power plants, ground granulated blast furnace slag (GGBFS) from iron production industry, and silica fume from silicon and ferrosilicon alloy industry are some examples of industrial wastes which are not only incorporable but also property enhancing replacements in cement.

Cement replacement is a helpful step towards sustainability in cement industry, but as the name implies, this process is mostly partial substitution rather than an alternative. Thus, it can be inferred that as long as portland cement clinker remains the main constituent of cement, any reduction to production related emissions will be limited. Therefore, fundamental changes in cement production are necessary and probably inevitable in the long term.

2.2 Low-Energy Cements

Cements which can be produced with reduced energy consumption relative to portland cement are called low-energy cements. This energy reduction may be achieved by lowering the clinkering temperature or by lowering the heat requirement for decomposition of raw meal ingredients.

Significant portion of energy consumption in cement production is due the calcination process. Decomposition of 1 ton of calcium carbonate requires 1782 GJ of energy (Odler, 2003). Required calcination energy can be reduced to some

extent by lowering the CaO amount in raw meal as in the case of low-C_3S and high-C_2S cements. Further reduction can be achieved by producing cement with constituents that contain calcium not in carbonated form in its structure.

Portland cement clinker is produced at ~1450 ^oC in order to obtain high amounts of C_3S, a significant contributor to both early age and later age strength upon hydration. By using alternative cementitious substances as the main strength contributor, production temperature can be lowered and substantial energy savings can be achieved. Calcium sulfoaluminate cement, sulfobelite cement, alinite cement, and fluoralinite cement are some examples. Among them, this thesis is concerned with alinite cement.

2.3 Alinite

Being a calcium oxy-chloro-aluminosilicate, alinite is related to alite (tricalcium silicate) with the difference that Ca^{2+} and Mg^{2+} cations are balanced by SiO_4^{4-} , AlO_4^{5-}, O^{2-} and Cl^- anions in alinite's structure unlike alite's, where Ca^{2+} cations are balanced by SiO_4^{4-} and O^{2-} anions (Odler, 2003). In crystallographic studies, it is revealed that particular position of chlorine atoms surrounded by eight calcium atoms is the main characteristic of alinite phase (Noudelman and Gadaev, 1986).

Hydration rate of alinite is significantly higher than that of alite. Comparison of hydration rates at early ages of hydration is shown below.

Table 1: Comparison of Rate of Hydration of Alite and Alinite (Odler, 2003).

Hydration time	**Degree of hydration (%)**		
	Alite	Alinite (Boikova et al., 1986)	Alinite (Ji et al., 1997)
15 min	-	-	9
1 h	10	22	-
6 h	15	64	36
12 h	20	70	-
1 d	25	80	43
3 d	40	85	53
28 d	-	-	62

Several researchers studied chemical composition of alinite, and different formulas have been proposed. It appears that alinite has no definite composition; however, it can be expressed with the following formula:

$$Ca_{10}Mg_{1-\frac{x}{2}}\square_{\frac{x}{2}}[(SiO_4)_{3+x}(AlO_4)_{1-x}]O_2Cl \quad (3)$$

where 0.35<x<0.45 and □ means a lattice vacancy (Neubauer & Pöllmann, 1994). Lattice structure of alinite appears to be relatively insensitive to impurities and may accommodate ions such as Fe^{3+}, P^{5+}, Ti^{4+}, Na^{+}, and K^{+} (Noudelman et al., 1980), which makes it a suitable candidate for waste utilization in cementitious systems.

2.4 Alinite Cement

The most important characteristic of alinite cement is its chlorine bearing composition. Phase composition of a typical alinite clinker is tabulated below.

Table 2: Phase Composition of Alinite Clinker (Odler, 2003).

Phase	**weight%**
Alinite	50-80
Belite	10-40
Calcium Aluminochloride	5-10
Calcium Aluminoferrite	2-10

Gypsum is not used to control setting time of the alinite cement. However, in this study as well, it is observed that intergrinding of gypsum with the clinker increases both early and ultimate strength of the cement (Pradip et al., 1990).

Chlorine is a constituent of main phases in alinite cement. It improves burnability of the mix and formation of alinite and belite along with sufficiently low free lime around 1000°C, which is significantly lower than ordinary portland cement (Singh et al., 2008).

Chloride ions are also found to decrease the crystal size of alinite, which improves hydration rate of alinite particles (Ftikos & Kiatos, 1994).

Some studies reveal that magnesium plays an important role in alinite formation. A minimum amount of 1-2% MgO need to be present for alinite synthesis (Singh et al., 2008). Magnesium compounds lower the decarbonation temperature from 825^{o}C to 775^{o}C and up to 3-4%, MgO increases alinite formation as well as stabilizing the phase (Ftikos et al., 1993; Singh et al., 2008). Higher amounts are undesirable since it leads to noticeable belinite formation, which forms at temperatures (~810^{o}C) below alinite (>1000^{o}C) and have poor hydraulic characteristics (Ruilun et al., 1984)

2.5 Solvay Process and Soda Waste Sludge

Soda ash is an important industrial product that is used in glass, detergent, steel, chemical industries and in various other applications. Its production amounts to more than 51 million tons a year (U.S. Geological Survey, 2016). Since the end of 20th century, the Solvay process has been the primary method of soda ash production in much of the world, due to the abundance of raw materials and relatively low environmental impact. Reactions of this process are shown in Figure 1.

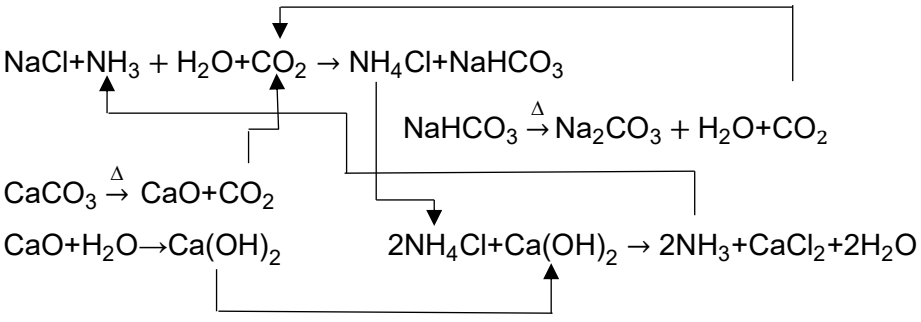

Figure 1: Chemical reactions of Solvay process(Gao et al., 2007).

The overall reaction can be interpreted as:

$$2NaCl + CaCO_3 \rightarrow Na_2CO_3 + CaCl_2 \quad (4)$$

or

$$\text{Brine} + \text{Limestone} \rightarrow \text{Soda ash} + \text{Soda waste}$$

Soda ash is taken for industrial applications while soda waste is discharged to rivers or settling ponds. Due to the mechanism of the process, waste comes out as an aqueous solution. Tighter environmental regulations obstruct uncontrolled disposal of the waste and increase the cost of storing. Hence, utilization of this waste has an economical aspect beside an environmental one.

CHAPTER 3

EXPERIMENTAL

3.1 Method

Within the scope of this study, alinite cement was produced from soda waste sludge to check its usability in a cementitious system. Raw mix recipes were determined according to lime saturation factor and lime index, considering raw materials' chemical compositions. Raw mixes were kneaded into cylindrical rods with addition of small amounts of water. They were then fed into a furnace on a refractory. From each mix, clinkers were produced with different maximum burning temperatures. Chosen samples were then produced with different calcination times (burning time at maximum burning temperature). Sample codes are given in the form "mix number.maximum burning temperature in ^{o}C.calcination time in hours" for clinkers, and in addition, "+addition of gypsum %" for hydrated samples (e.g. A3.1150.2+6%). Chemical and mineralogical analyses of clinkers were made. Density and grindability of clinkers were also examined. Then, effects of amount of gypsum addition on various hydration properties were observed with normal consistency, setting time, compressive strength, calorimeter, and powder XRD tests and scanning electron microscopy (SEM). Tests were performed in Research and Development Laboratories of Turkish Cement Manufacturers' Association, METU Central Laboratory, and METU Civil Engineering Department Materials of Construction Laboratory.

3.2 Raw Materials

The waste was provided by Şişecam Soda Sanayii A.Ş Mersin Soda Plant. It was delivered in unprocessed form. Unfortunately, the fact that oven dry sample contains almost 25% chlorine undermines the effective use of unprocessed form as the only calcium source.

Alinite cement can be produced from raw materials which contain limestone, clay, MgO and $CaCl_2$ (Tokyay, 2016). Apart from the soda waste sludge, raw materials necessary for experiments was obtained from Votorantim Çimento A.Ş. Hasanoğlan Cement Plant.

3.3 Raw Mix Proportioning

Chemical compositions of raw materials were necessary to adjust raw mix proportions. Results of chemical analyses of raw materials, which is conducted in Turkish Cement Manufacturers' Association's laboratory, are presented in Table 3.

Table 3: Chemical Compositions of Raw Materials.

Composition	**Limestone**	**Clay**	**Iron Ore**	**SWS (dried)**	**Gypsum Rock**
LOI,%	42.73	9.89	11.7	24.85	18.9
SiO_2, %	1.97	56.91	23.09	8.23	8.36
Al_2O_3, %	0.68	14.65	3.92	1.82	1.96
Fe_2O_3, %	0.23	6.22	55.42	1.11	1.09
CaO, %	53.24	5.19	1.25	30.74	30.34
MgO, %	1.07	2.45	1.07	0.49	0.5
SO_3, %	<0.01	0.01	0.24	2.48	37.74
Na_2O, %	0.09	0.84	0.2	3.8	0.06
K_2O, %	0.05	1.94	0.18	0.36	0.33
TiO_2, %	-	0.84	0.07	0.13	0.14
P_2O_5, %	-	0.1	0.02	0.03	0.03
Cr_2O_3, %	-	0.17	1.94	0.02	0.01
Mn_2O_3, %	-	0.15	0.18	0.04	0.03
Cl^- , %	0.0064	0.0102	0.0226	24.92	-
Density, g/cm^3	2.72	2.59	3.26	2.40	2.41

One of the major parameters to consider in raw mix proportioning is lime saturation factor (LSF). LSF is used to determine the compound forming capacity of calcium oxide with other major oxides present and the ratio of alite to belite in the clinker. It is calculated as:

$$\mathrm{LSF} = \frac{100 \times \%\mathrm{CaO}}{2.80\%\mathrm{SiO_2} + 1.18\%\mathrm{Al_2O_3} + 0.65\%\mathrm{Fe_2O_3}} \quad (5)$$

Complete lime saturation (LSF = 100) means theoretically all calcium oxide is combined as C_3S, C_3A, and C_4AF, assuming there is no free lime remained. The higher the LSF, the more will be the amount of C_3S. For ordinary portland cement, this value is generally between 90-95 and for high early strength cement, it is

around 95-98 (Duda, 1988). In the case of alinite cement clinker, a chlorine modified formula is proposed as (Ftikos et al., 1993):

$$\mathrm{LSF_{mod}} = \frac{100 \times (\%\mathrm{CaO} - 0.789\%\mathrm{Cl})}{2.80\%\mathrm{SiO_2} + 1.18\%\mathrm{Al_2O_3} + 0.65\%\mathrm{Fe_2O_3}} \quad (6)$$

It is stated that $\mathrm{LSF_{mod}}$ values greater than 80 result in reduced burnability and inhibition of alinite formation (Ftikos et al., 1993).

Another parameter called lime index (LI) should also be considered in raw mix design of alinite cement. It is the ratio of calcium oxide to the sum of silica, alumina, and ferrite oxides in the mix by weight:

$$\mathrm{LI} = \frac{\%\mathrm{CaO}}{\%\mathrm{SiO_2} + \%\mathrm{Al_2O_3} + \%\mathrm{Fe_2O_3}} \quad (7)$$

For a measureable strength, lime index should not be less than 1.5, and results improve linearly up to 1.8, as can be seen from figure 2 (Pradip et al., 1990).

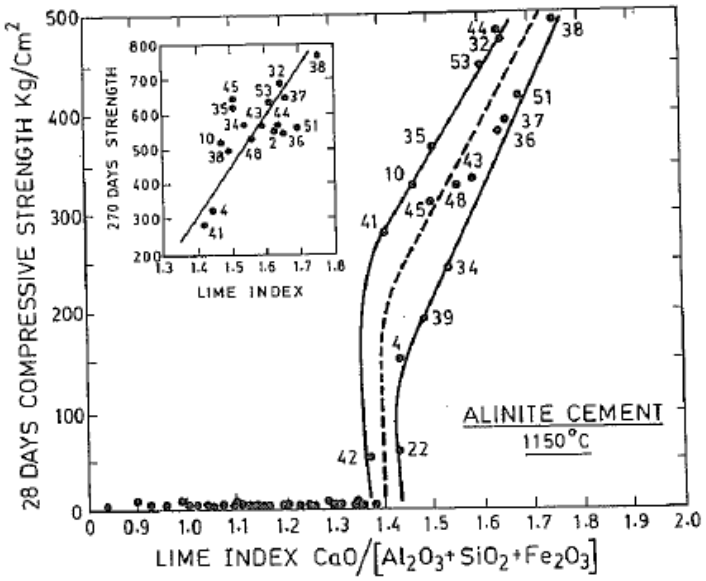

Figure 2: Lime index versus compressive strength graph (Pradip et al., 1990).

When soda waste sludge is dried in its original form without any filtration process, resulting chlorine content is too high. Therefore some mixes were prepared as partial replacement of limestone with soda waste sludge. In this study, one mix with soda waste sludge as the only calcium source is prepared. Also, a portland cement mix with a suitable LSF is calculated and limestone is replaced with 30% and 50% soda waste sludge, by mass. Raw meal compositions of mixes are as follows:

Table 4: Recipes of Raw Mixes.

Mix	Limestone	Soda Waste Sludge	Clay	Iron ore
C	78.91	0	20.61	1.30
A1	0	76.91	22.28	0.80
A2	54.66	23.43	20.61	1.30
A3	39.04	39.04	20.61	1.30

In the table, A1 denotes the mix with soda solid waste as the only calcium source, and A2 and A3 denotes 30% - 50% replacement of limestone with soda waste

sludge, respectively. C is the control portland cement produced in laboratory with traditional raw materials to compare some physical properties.

3.4 Burning Regime

In order to determine burning regime, 2 different maximum burning temperature were selected, considering the literature (Kesim et al., 2013; Mowla et al., 1999). Total of 6 samples were prepared with 1 hour of calcination time, namely A1.1050.1, A1.1150.1, A2.1050.1, A2.1150.1, A3.1050.1, and A3.1150.1. After chemical analyses, additional 4 samples are prepared with different calcination times, namely A2.1150.2, A2.1150.4, A3.1150.2, and A3.1150.4.

3.5 Tests on Alinite Clinker

Prepared clinkers were sent to Turkish Cement Manufacturers' Association's laboratory for chemical and mineralogical analyses. Their physical properties were determined in the Materials of Construction Laboratory of METU.

3.5.1 Physical Properties

One of the possible advantages of alinite cement is its easier grindability. To validate this, portland cement clinker and alinite cement clinker were ground in a ball mill to same Blaine fineness values, and grinding energy was recorded. Density of ground clinkers were calculated according to ASTM (ASTM C188-15, 2015). Fineness of ground clinkers were then calculated according to EN 196-6 (EN 196-6, 2010).

3.5.2 Chemical Analyses

Oxide compositions in clinkers were determined as well as loss on ignition values and chlorine and free calcium oxide content. Chemical analyses results of clinkers were found using UV spectrophotometry, ICP-OES, acidimetric glycol method and EN 196-2 (EN 196-2, 2010).

3.5.3 Mineralogical Analyses

Clinkers coded A1.1050.1, A1.1150.1, A2.1050.1, A2.1150.1, A2.1150.2, A2.1150.4, A3.1050.1, A3.1150.1, A3.1150.2, A3.1150.4 were sent to Turkish Cement Manufacturers' Association laboratory for mineralogical analysis. Mineralogical analyses of clinkers were performed with a Philips brand device by using X-Ray Diffraction (XRD) method.

3.6 Tests on Hydrated Alinite Cement

Selected samples were produced in bigger quantities for testing. Their hydration processes were investigated by XRD, SEM, and calorimetry methods as well as setting time and strength tests.

3.6.1 Normal Consistency and Setting Time

Effects of gypsum addition on setting time and normal consistency of A3.1150.2 samples were observed up to 12%. Normal consistency and setting time tests of samples were performed according to EN 196-3 (EN 196-3:2005+A1:2008, 2008).

3.6.2 Compressive Strength

Effects of fineness, calcination time, and gypsum addition on compressive strength of alinite cement mortars were determined by measuring 2-7-28-Day strength values according to EN 196-1 (EN 196-1, 2009). 90 days strength of A2.1150.2+6% Gypsum, A3.1150.2+6% Gypsum, A3.1150.2+12% Gypsum, A3.1150.4+6% Gypsum samples were also detected to monitor hydration in the long term. Unless stated otherwise, all compressive strength results are average of 4 samples. UTEST testing instrument with 250kN ultimate capacity was used as universal testing machine and rate of loading of 1.5kN/s was applied.

3.6.3 Calorimeter

TAM Air Isothermal Calorimeter was used for calorimeter tests. A2.1150.2 without gypsum addition, A2.1150.2+6% gypsum, A2.1150.2+12% gypsum,

A3.1150.2 without gypsum addition, A3.1150.2+3% gypsum, A3.1150.2+6% gypsum, A3.1150.2+9% gypsum, and A3.1150.2+12% gypsum were tested and compared to a commercially available PC.

3.6.4 X-Ray Diffraction

Mineralogical analyses of hydrated samples were done by a powder X-Ray Diffractometer. A fraction of sample was sieved through a 150 μm (#100) mesh and put into vibration chamber. Olympus BTX-II model equipment was used in testing. Device allows measurements up to 55^{o} 2θ angle of diffraction. Resulting X-Ray Diffraction data was obtained in a graphical form. By matching peaks in the diffractograms with individual peaks of various minerals, corresponding mineral phases were identified.

3.6.5 Scanning Electron Microscopy (SEM)

Composition and crystal formations on the surface of hydrated pastes were monitored with scanning electron microscope. Imaging was performed in METU Central Laboratory with “FEI Quanta 400F” model microscope.

CHAPTER 4

RESULTS AND DISCUSSION

4.1 Raw Materials and Raw Mix

Resulting chemical compositions of raw mixes, as well as lime saturation factors and lime indexes, are presented in table 5.

Table 5: Chemical Compositions of the Raw Mixes.

Content	**C**	**A1**	**A2**	**A3**
LOI	35.56	21.41	31.37	28.58
SiO_2, %	13.57	19.19	15.03	16.01
Al_2O_3, %	3.60	4.70	3.87	4.05
Fe_2O_3, %	2.18	2.68	2.39	2.53
CaO, %	42.66	24.81	37.39	33.88
MgO, %	1.35	0.93	1.22	1.13
SO_3, %	0.01	1.91	0.59	0.97
Na_2O, %	0.25	3.11	1.12	1.69
K_2O, %	0.44	0.71	0.51	0.56
TiO_2, %	0.17	0.29	0.20	0.22
P_2O_5, %	0.02	0.05	0.03	0.03
Cr_2O_3, %	0.06	0.07	0.06	0.07
Mn_2O_3, %	0.03	0.07	0.04	0.05
Cl^- , %	0.01	19.17	5.84	9.73
LSF_{mod}	97.70	15.87	67.98	51.11
LI	2.20	0.93	1.76	1.50

4.2 Alinite Clinker Properties

4.2.1 Chemical Properties

Chemical analyses results of A1, A2, A3 clinkers with 1050°C and 1150°C maximum burning temperature and 1 hour of calcination time are presented in Table 6.

Table 6: Chemical Analysis Results of Clinkers with Different Maximum Burning Temperatures.

Content	**C (1450)**	**A1. 1050.1**	**A1. 1150.1**	**A2. 1050.1**	**A2. 1150.1**	**A3. 1050.1**	**A3. 1150.1**
LOI	0.32	5.51	5.26	2.78	1.16	2.29	1.53
SiO_2	21.61	18.00	19.09	20.36	21.19	19.63	20.23
Al_2O_3	5.11	5.00	5.04	5.04	5.20	4.98	5.07
Fe_2O_3	3.32	2.45	2.53	3.02	3.24	2.78	3.06
CaO	67.02	40.55	40.90	57.80	60.38	53.00	53.40
MgO	2.11	2.40	2.31	2.24	2.25	2.29	2.25
SO_3	0.03	2.41	2.61	1.00	0.92	1.53	1.57
Na_2O	0.24	4.00	3.82	0.91	0.22	2.85	1.60
K_2O	0.06	0.36	0.32	0.27	0.14	0.36	0.27
Cl^-	0.02	19.27	18.08	6.63	4.93	10.42	10.15
Free CaO	2.68	0.15	0.14	8.25	2.86	3.89	0.86

These results show that 1150°C maximum burning temperature provides better properties for all samples. It is observed that A1 mix melted at both temperatures, leaving only a small portion of it available for analysis; and that portion is not suitable as a clinker due to its low CaO content, high LOI and alkali oxide content. Also, its chlorine content is very high, even for alinite cement clinker. Effects of different calcination times are investigated for A2.1150 and A3.1150. Chemical analyses results of 2 hours and 4 hours of calcination time are shown in Table 7.

Table 7: Chemical Analysis Results of Clinkers with Different Calcination Times.

Content	A2. 1150.2	A2. 1150.4	A3. 1150.2	A3. 1150.4
LOI	1.98	2.40	3.63	2.25
SiO_2	21.22	20.97	19.87	20.55
Al_2O_3	5.13	5.09	4.99	5.17
Fe_2O_3	3.23	3.09	3.08	3.30
CaO	59.77	59.65	54.29	55.14
MgO	2.24	2.27	2.20	2.27
SO_3	1.06	0.99	1.65	1.36
Na_2O	0.22	0.03	0.88	0.84
K_2O	<0.01	<0.01	0.13	0.16
Cl^-	4.40	5.42	9.14	8.90
Free CaO	0.68	0.39	0.67	0.60

Loss on ignition values vary probably due to different levels of exposure to air. Free CaO content shows that A2 requires at least 2 hours of calcination time for better clinkerization. Although there is a slight improvement with increasing calcination time, the free CaO content of A3 is acceptable after 1 hour. Alkali (Na_2O and K_2O) content of A2 is acceptable for all samples. Alkali content of A3 is relatively high, and it can be said that calcination time should not be less than 2 hours as far as alkalis are concerned, which would still require expansion check against alkali-aggregate reaction. In alinite cement, some chlorine is bound within hydration products, so the water soluble chloride ion content in the final product is the decisive parameter in determining corrosion susceptibility, rather than the chlorine content in the clinker.

4.2.2 Mineralogical Properties

Mineralogical properties were determined with X-Ray Diffractometer. XRD patterns and mineral phases of A2.1150.2 and A3.1150.2 are presented in figure 3 and 4. Rest of phases and diffractograms of samples are provided in Appendix A.

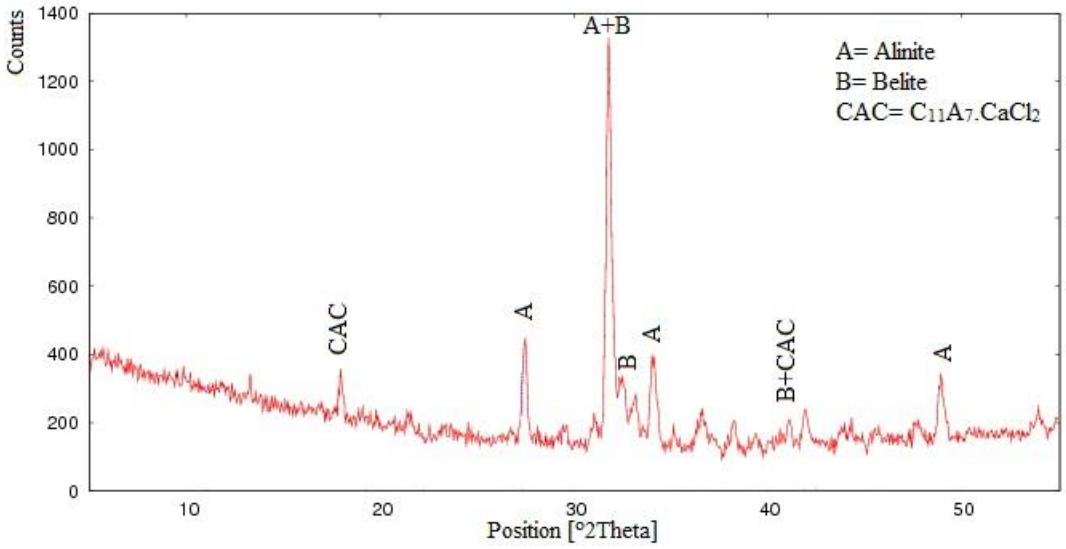

Figure 3: XRD pattern of A2.1150.2.

A2.1150.2
Alinite [$Ca_{10}Mg_{0.8}[(SiO_4)_{3.4}(AlO_4)_{0.6}]O_2Cl$]
Belite [C_2S]
Calcium Aluminochloride [$C_{11}A_7CaCl_2$]

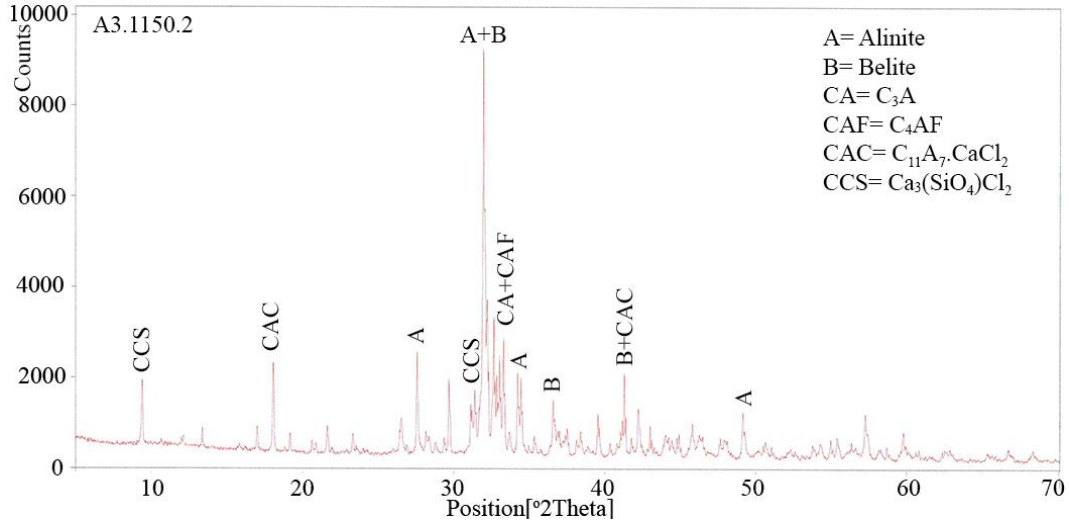

Figure 4: XRD pattern of A3.1150.2.

A3.1150.2
Alinite [$Ca_{10}Mg_{0.8}[(SiO_4)_{3.4}(AlO_4)_{0.6}]O_2Cl$]
Belite [C_2S]
Aluminate [C_3A]
Ferrite [C_4AF]
Calcium Aluminochloride [$C_{11}A_7CaCl_2$]
Calcium Chloride Silicate [$Ca_3(SiO_4)Cl_2$]

It is observed that cementitious phases similar to ordinary portland cement are present in alinite cement clinker, with the difference that alite phase is replaced by alinite phase, and calcium chloride silicates are also observed. Alinite and belite were the major phases.

4.2.3 Physical Properties

In order to measure Blaine fineness values, density of clinkers need to be determined. Density of ground alinite cement clinkers and portland cement clinker are shown in table 8.

Table 8: Density Values of Clinkers.

Sample	Density (g/cm^3)
C	3.26
A2.1150	3.03
A3.1150	3.00

While there is not much difference between alinite cement clinkers, they both have lower density than portland cement clinker.

Clinkers were fed into ball mill in either 5 kg or 2.5 kg batches. Grinding energy per minute did not change with different clinkers. This is attributed to the fact that mass of clinker takes up a small portion of total ball mill mass, so majority of the

energy is spent to rotate the mill and steel balls. Therefore, required grinding energy is proportional to time of grinding.

Table 9: Time of Grinding of Clinkers with 5 kg Batches

Sample (5kg)	To Blaine = 3500 cm^2/g	To Blaine = 5000 cm^2/g
C	195 min	
A3.1150.2	60 min	120 min
A3.1150.4	45 min	

Table 10: Time of Grinding of Clinkers with 2.5 kg Batches

Sample (2.5kg)	To Blaine = 5000 cm^2/g
A2.1150.2	50 min
A3.1150.2	45 min

Results show that alinite cement clinker requires significantly less energy than portland cement clinker for grinding. Considering this dramatic difference and the fact that alinite cement in this research contains high belite (and therefore overall hydration will progress slowly), alinite cements are ground to 5000 cm^2/g Blaine fineness for further testing. Required grinding time for 5000 cm^2/g Blaine fineness was 120 minutes for A3.1150.2, still far less than C to reach 3500 cm^2/g Blaine fineness. A2.1150.2 was produced and ground in smaller quantities so direct comparison to PC was not possible, however, it was seen that grindability of it is similar to grindability of A3.1150.2.

4.3 Hydrated Alinite Cement Properties

To clarify hydration characteristics of alinite cement produced with soda waste sludge, results of normal consistency, setting time, calorimeter, compressive strength, and powder XRD tests along with scanning electron microscope images are presented in this section.

4.3.1 Physical Properties

Alinite cement's normal consistency and setting time with changing gypsum content was measured and compared to a commercially available portland cement.

Table 11: Normal Consistency and Setting Time of Alinite Cements and PC.

Sample	Normal Consistency w/c	Initial Setting (min)	Final Setting (min)
PC (CEM I 42.5R)	0.265	95	163
A2.1150.2+6%	0.235	17	32
A3.1150.2+3%	0.245	25	47
A3.1150.2+6%	0.240	24	46
A3.1150.2+9%	0.235	20	44
A3.1150.2+12%	0.230	18	42

It was observed that alinite cement paste requires less water content than portland cement does for the same consistency, regardless of its gypsum content. Water requirement slightly decreases with increasing gypsum content. This might be the result of decreasing clinker content.

Another finding is that alinite cement sets very rapidly relative to portland cement. This implies faster rate of hydration at the initial stage of hydration in the case of alinite cement, and this rate increases with increasing gypsum content. It is also worth noting that A2.1150.2+6% paste set even more rapid than A3.1150.2 pastes.

4.3.2 Calorimetric Results

Early rate of heat generation in A2 and A3 pastes with different gypsum content was monitored in order to observe effect of gypsum content on early hydration rate and to compare rate of reaction in alinite cement paste to that of portland cement.

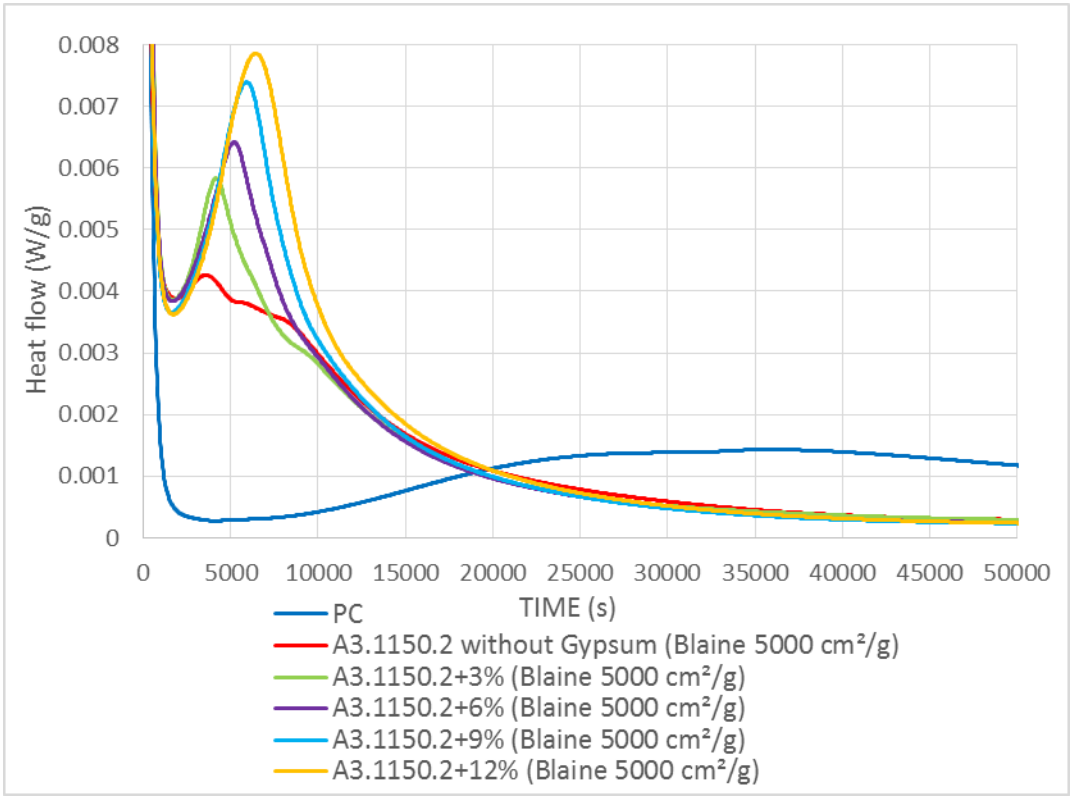

Figure 5: Heat flow curves of PC and A3 samples at early hydration stages.

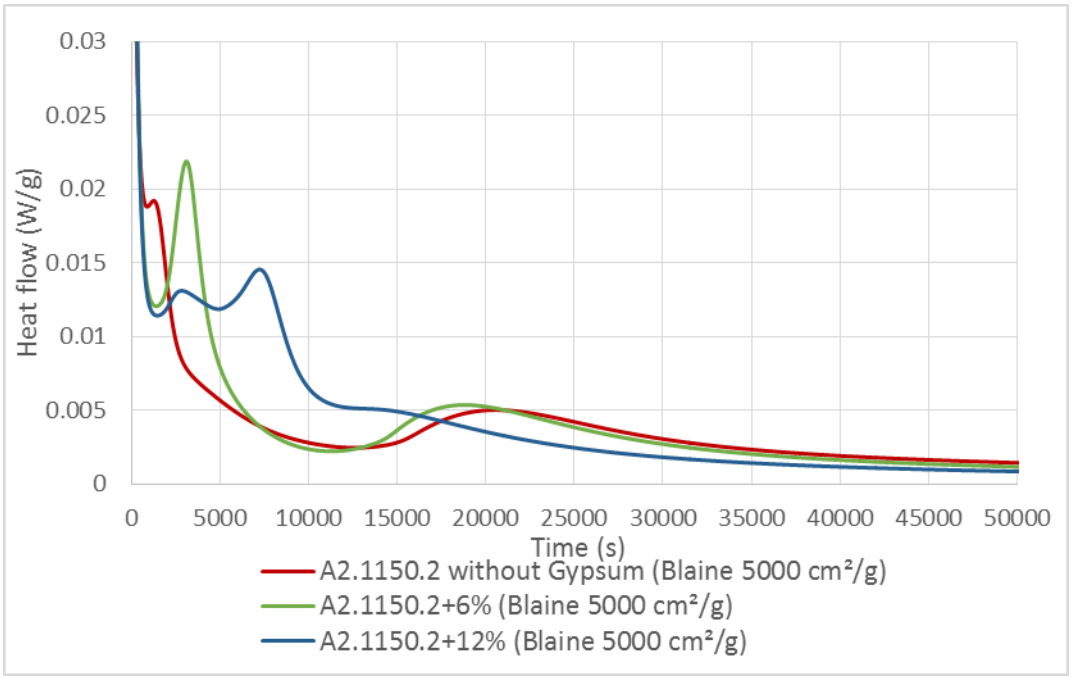

Figure 6: Heat flow curves of A2 samples at early hydration stages.

It is seen that dormant period, which is typical in portland cement, is not observed in alinite cement. This behavior can be explained with the argument that presence of calcium chloride within solution increases inner C-S-H formation by increasing diffusion of ions and water through outer C-S-H layer due to increased mean pore diameter (Juenger et al., 2005). In the case of A3 cement, increasing gypsum content resulted in higher peaks, implying higher reactivity. This is consistent with setting time results.

Situation in A2 is more complex. All three samples appear to have two common peaks. Increasing gypsum content seems to retard the former (second peak in the case of A2.1150.2+12% gypsum and first peak in other two) and accelerate the latter. First peak of A2.1150.2+12% gypsum sample might indicate a different reaction that takes place which is not present in the other two. These behaviors all require further investigation for explanation. In any case, rate of heat generation in A2 samples is significantly greater than both PC sample and A3 samples.

Total heat generation for the first days was also observed as an indication of overall hydration reactivity. Results are shown in figure 7 and 8.

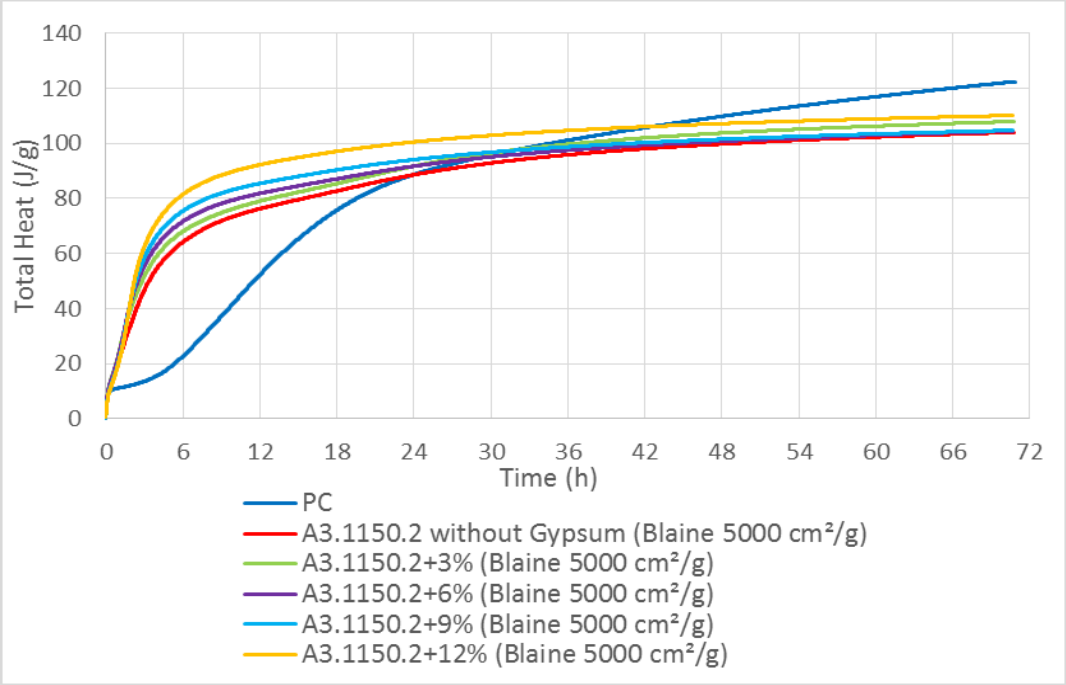

Figure 7: Total heat generation curves of PC and A3 samples.

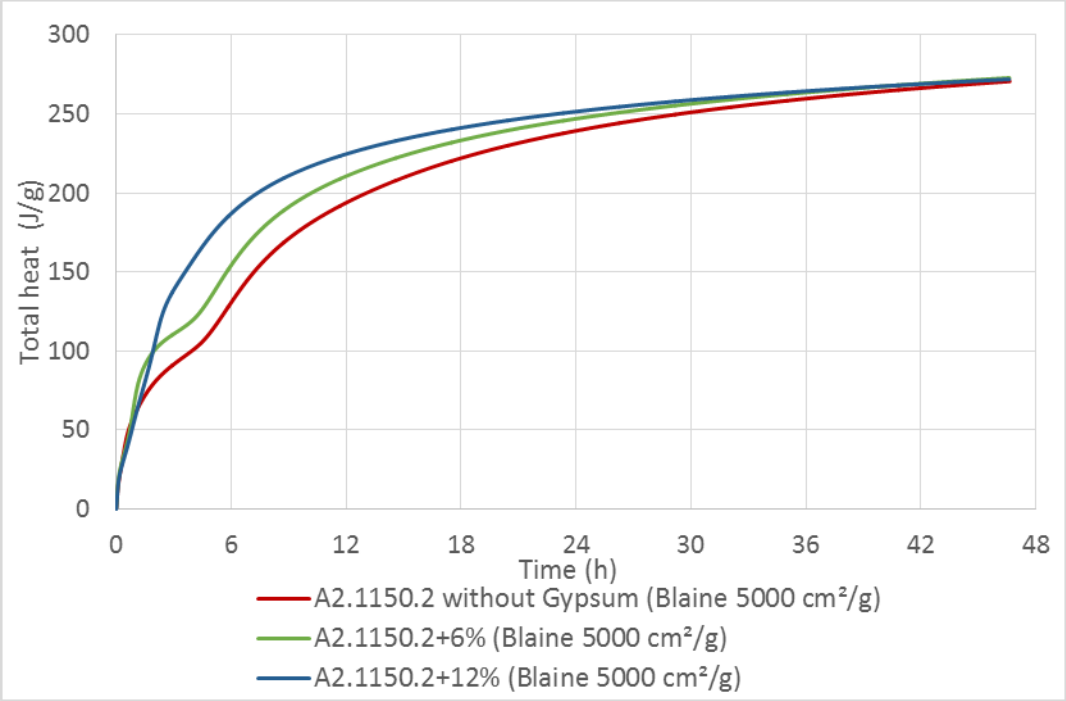

Figure 8: Total heat generation curves of A2 samples.

Heat generation of A3 samples increase with increasing gypsum content initially, but that correlation is lost after 1 day. Although lower at first, total heat generation of PC sample exceeds all of A3 samples after 2 days. All A2 samples generated approximately the same amount of heat at about 2 days, which is twice as much as PC sample.

4.3.3 Mechanical Properties

4.3.2.1 Effect of Fineness on Compressive Strength

Effect of fineness on compressive strength was investigated. A3.1150.4 clinker was used for this test since it had slightly better chemical composition than other A3 clinkers therefore expected to give better results.

Table 12: Effect of Fineness on Compressive Strength.

W/C = 0.5	Fineness (cm^2/g)	Compressive Strength (MPa)			
		2-Day	7-Day	28-Day	90-Day
A3.1150.4 + 6%	3500	6.4	9.3	16.7	30.8
	4500	7.7	10.9	19.1	*
	5000	10.1	12.2	21.7	*

* = was not performed due to lack of clinker

Compressive strength increases with increasing fineness, as expected. Strength difference due to fineness is expected to reduce at later ages of hydration, which is not the case in A3.1150.4+6% mortars at 28 days. It implies that considerable hydration takes place after 28 days. This is later confirmed by 90 days compressive strength result of sample which has 3500 cm^2/g specific surface area.

4.3.2.2 Effect of Calcination Time on Compressive Strength

In order to understand the effect of calcination time on compressive strength, mortars were prepared with A3 clinkers that have different calcination times, and 2,7, and 28 days strengths were determined.

Table 13: Effect of Calcination Time of Clinker on Compressive Strength.

W/C = 0.5 Fineness= 5000 cm^2/g	Compressive Strength (MPa)		
Sample	2-Day	7-Day	28-Day
A3.1150.1+6%	9.0	12.3	21.0
A3.1150.2+6%	9.0	12.3	20.6
A3.1150.3+6%	10.2	12.6	21.7
A3.1150.4+6%	10.1	12.2	21.7

It is observed that strength results are not affected by calcination time, therefore A3.1150.2 is selected for further testing, considering its lower free CaO and alkali oxides (Na_2O, K_2O) content relative to A3.1150.1.

4.3.2.3 Effect of Water/Cement ratio on Compressive Strength

During preliminary tests, it was noticed that alinite cement mortar is considerably more flowable than portland cement mortar when the same water/cement ratio is used. Hence, effect of water/cement ratio on flowability was measured according to ASTM (ASTM C1437-15, 2015) and presented in table 14.

Table 14: Effect of Water/Cement Ratio on Flowability

Sample	**Flow (%)**
PC (CEM I 42.5R)-w/c = 0.50	50
A3.1150.2+6%-w/c=0.50	120
A3.1150.2+6%-w/c=0.43	70
A3.1150.2+6%-w/c=0.40	50
A3.1150.2+6%-w/c=0.30	0

Compressive strength results of A3.1150.2 cement mortars with different water/cement ratios are presented in table 15.

Table 15: Effect of Water/Cement Ratio on Compressive Strength.

Fineness= 5000 cm^2/g	**Compressive Strength (MPa)**		
Sample	**2-Day**	**7-Day**	**28-Day**
A3.1150.2+6%-w/c=0.50	8.7	12.7	22.7
A3.1150.2+6%-w/c=0.40	12.9	16.8	26.5
A3.1150.2+6%-w/c=0.30	5.9	6.6	10.2

As expected, 0.5 water/cement ratio results in lower strength values due to higher capillary porosity. Sample with 0.3 water/cement ratio was too stiff to be compacted adequately. Therefore, 0.4 water/cement ratio is selected for further testing due to flowability comparable to portland cement with 0.5 water/cement ratio and strength results superior to other samples.

4.3.2.4 Effect of Gypsum Content on Compressive Strength

As part of investigation of interaction between alinite cement and gypsum, A3 cement mortars were prepared with different gypsum additions. Their compressive strength results along with A2 cement's and commercially available portland cement's results are presented in table 16.

Table 16: Effect of Gypsum Content on Compressive Strength.

Fineness = 5000 cm^2/g	**Compressive Strength (MPa)**			
w/c = 0.4				
Sample	**2-Day**	**7-Day**	**28-Day**	**90-Day**
PC	21.0	35.2	45.8	53.8
A2.1150.2+6%	22.3	30.7	42.3	46.7
A3.1150.2+3%	10.9	15.4	23.2	-
A3.1150.2+6%	11.7	15.9	24.2	36.6
A3.1150.2+9%	12.8	16.7	25.0	-
A3.1150.2+12%	14.7	19	29.2	39.4
A3.1150.2+15%	16.7	18.7	30.9	-

These results show that compressive strength of A3 cement increases with increasing gypsum content up to 15% addition. However, sample with %15 gypsum addition had lower flowability relative to other alinite cement samples, which had flowability similar to control portland cement. More water could be added to that sample to adjust flowability, but it would undermine the reason of gypsum addition by reducing strength due to increased water/cement ratio.

It is seen that strength results comparable to that of portland cement can be attained with A2 mix. Since there was not enough A2 clinker, however, effect of gypsum content on compressive strength of A2 mortars could not be observed.

4.3.4 Mineralogical Properties

Hydration products of A2.1150.2+6% and A3.1150.2+6% pastes were monitored with powder XRD method. 2 hours, 6 hours, 2 days, and 28 days results of A2.1150.2+6% and A3.1150.2+6% pastes are presented in figure 9 to 18. 90 days results of A3.1150.2+6% and A3.1150.2+12% are also present for comparison.

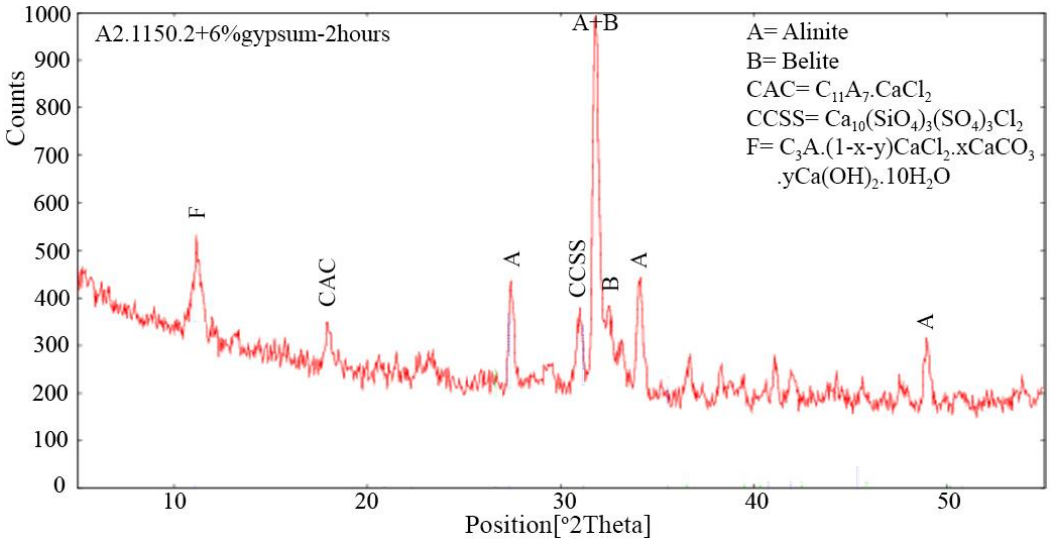

Figure 9: XRD Pattern of paste of A2.1150.2+6% at 2 hours.

A2.1150.2+6% paste – 2 hours
Alinite [$Ca_{10}Mg_{0.8}[(SiO_4)_{3.4}(AlO_4)_{0.6}]O_2Cl$]
Belite [C_2S]
Calcium Aluminochloride [$C_{11}A_7CaCl_2$]
Calcium Chloride Silicate Sulfate [$Ca_{10}(SiO_4)_3(SO_4)_3Cl_2$]
Friedel's salt [$C_3A.(1-x-y)CaCl_2.xCaCO_3.yCa(OH)_2.10H_2O$]

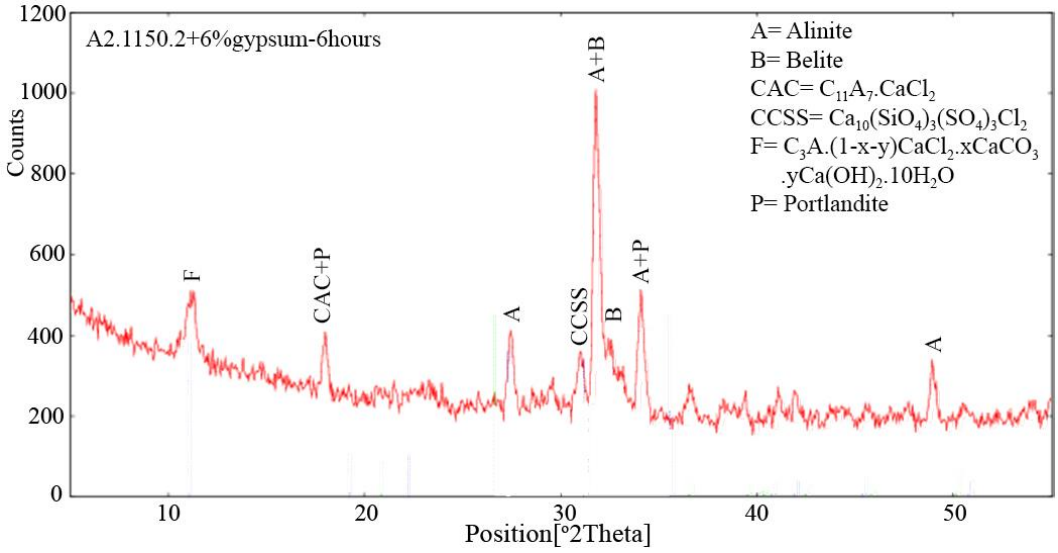

Figure 10: XRD Pattern of paste of A2.1150.2+6% at 6 hours.

A2.1150.2+6% paste – 6 hours
Alinite [$Ca_{10}Mg_{0.8}[(SiO_4)_{3.4}(AlO_4)_{0.6}]O_2Cl$]
Belite [C_2S]
Calcium Aluminochloride [$C_{11}A_7CaCl_2$]
Calcium Chloride Silicate Sulfate [$Ca_{10}(SiO_4)_3(SO_4)_3Cl_2$]
Friedel's salt [$C_3A.(1-x-y)CaCl_2.xCaCO_3.yCa(OH)_2.10H_2O$]
Portlandite [$Ca(OH)_2$]

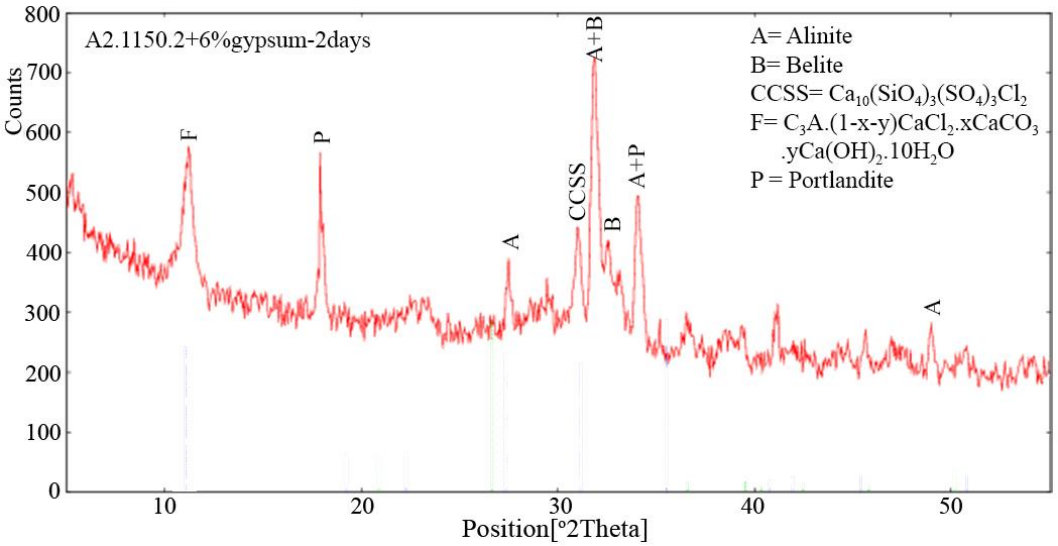

Figure 11: XRD Pattern of paste of A2.1150.2+6% at 2 days.

A2.1150.2+6% paste – 2 days
Alinite [$Ca_{10}Mg_{0.8}[(SiO_4)_{3.4}(AlO_4)_{0.6}]O_2Cl$]
Belite [C_2S]
Calcium Chloride Silicate Sulfate [$Ca_{10}(SiO_4)_3(SO_4)_3Cl_2$]
Friedel's salt [$C_3A.(1\text{-}x\text{-}y)CaCl_2.xCaCO_3.yCa(OH)_2.10H_2O$]
Portlandite [$Ca(OH)_2$]

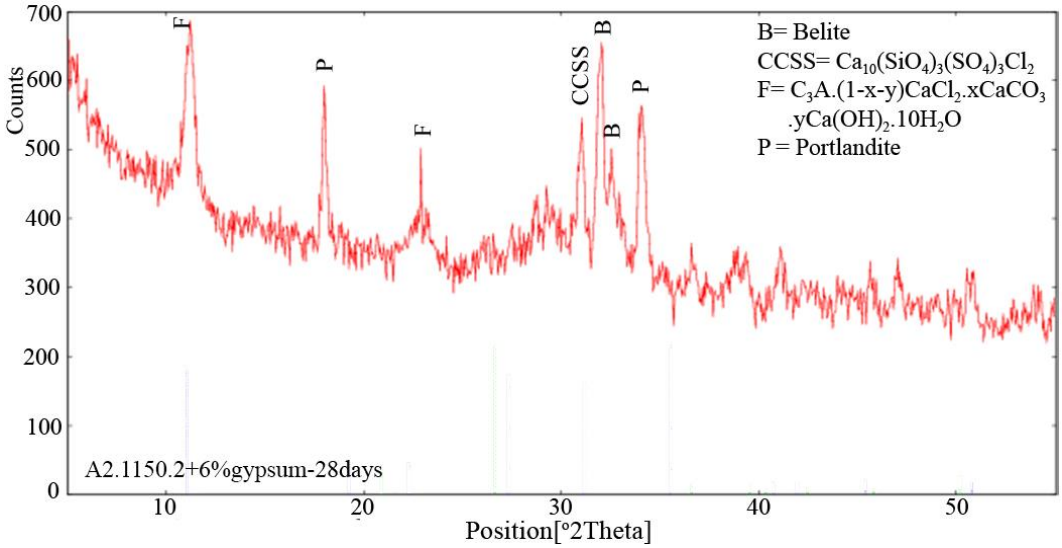

Figure 12: XRD Pattern of paste of A2.1150.2+6% at 28 days.

A2.1150.2+6% paste – 28 days
Alinite [$Ca_{10}Mg_{0.8}[(SiO_4)_{3.4}(AlO_4)_{0.6}]O_2Cl$]
Belite [C_2S]
Calcium Chloride Silicate Sulfate [$Ca_{10}(SiO_4)_3(SO_4)_3Cl_2$]
Friedel's salt [$C_3A.(1\text{-}x\text{-}y)CaCl_2.xCaCO_3.yCa(OH)_2.10H_2O$]
Portlandite [$Ca(OH)_2$]

It is determined that Friedel's salt-like phase [$C_3A.(1\text{-}x\text{-}y)CaCl_2.xCaCO_3$ $.yCa(OH)_2.10H_2O$], as suggested by Neubauer and Pöllmann (Neubauer & Pöllmann, 1994), is noticeable starting from 2 hours of hydration.

Calcium hydroxide, which is also a part of Friedel's salt-like phase, was observed individually after 6 hours of hydration. This confirms that main hydration reaction, which results in formation of C-S-H and calcium hydroxide, takes place in alinite cement hydration.

The peak of calcium chloride silicate [$Ca_3(SiO_4)Cl_2$] around 31°2Theta appears steadily throughout hydration. This implies a product with the same peak is produced while calcium chloride silicate is consumed. A study on this subject that uses a similar waste also encountered the same peak and identified it as calcium chloride silicate sulfate [$Ca_{10}(SiO_4)_3(SO_4)_3Cl_2$] (Kesim et al., 2013). When similarities between constituents are considered, this proposal is found valid.

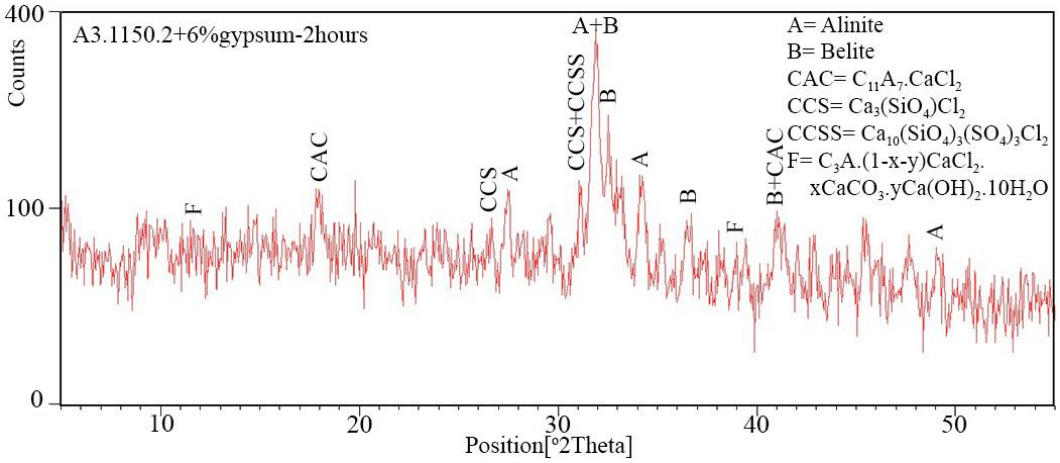

Figure 13: XRD Pattern of paste of A3.1150.2+6% at 2 hours.

A3.1150.2+6% paste – 2 hours
Alinite [$Ca_{10}Mg_{0.8}[(SiO_4)_{3.4}(AlO_4)_{0.6}]O_2Cl$]
Belite [C_2S]
Calcium Aluminochloride [$C_{11}A_7CaCl_2$]
Calcium Chloride Silicate [$Ca_3(SiO_4)Cl_2$]
Calcium Chloride Silicate Sulfate [$Ca_{10}(SiO_4)_3(SO_4)_3Cl_2$]
Friedel's salt [$C_3A.(1\text{-}x\text{-}y)CaCl_2.xCaCO_3.yCa(OH)_2.10H_2O$]

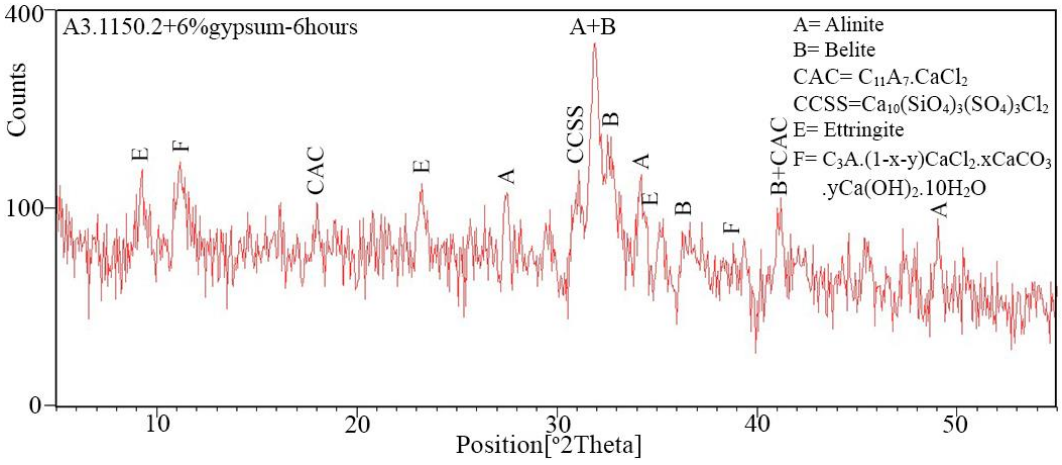

Figure 14: XRD Pattern of paste of A3.1150.2+6% at 6 hours.

A3.1150.2+6% paste – 6 hours
Alinite [$Ca_{10}Mg_{0.8}[(SiO_4)_{3.4}(AlO_4)_{0.6}]O_2Cl$]
Belite [C_2S]
Calcium Aluminochloride [$C_{11}A_7CaCl_2$]
Calcium Chloride Silicate Sulfate [$Ca_{10}(SiO_4)_3(SO_4)_3Cl_2$]
Ettringite [$C_3A.(CaSO_4)_3.32H_2O$]
Friedel's salt [$C_3A.(1\text{-}x\text{-}y)CaCl_2.xCaCO_3.yCa(OH)_2.10H_2O$]

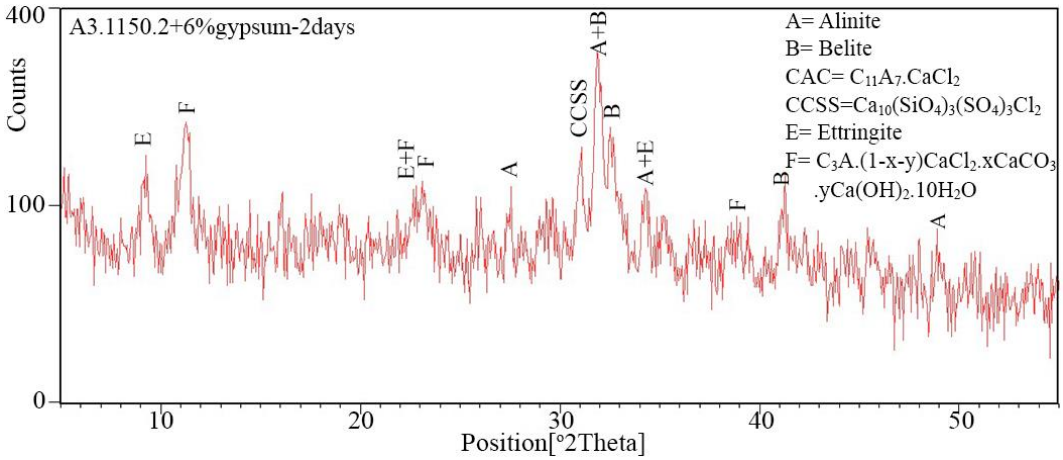

Figure 15: XRD Pattern of paste of A3.1150.2+6% at 2 days.

A3.1150.2+6% paste – 2 days
Alinite [$Ca_{10}Mg_{0.8}[(SiO_4)_{3.4}(AlO_4)_{0.6}]O_2Cl$]
Belite [C_2S]
Calcium Aluminochloride [$C_{11}A_7CaCl_2$]
Calcium Chloride Silicate Sulfate [$Ca_{10}(SiO_4)_3(SO_4)_3Cl_2$]
Ettringite [$C_3A.(CaSO_4)_3.32H_2O$]
Friedel's salt [$C_3A.(1\text{-}x\text{-}y)CaCl_2.xCaCO_3.yCa(OH)_2.10H_2O$]

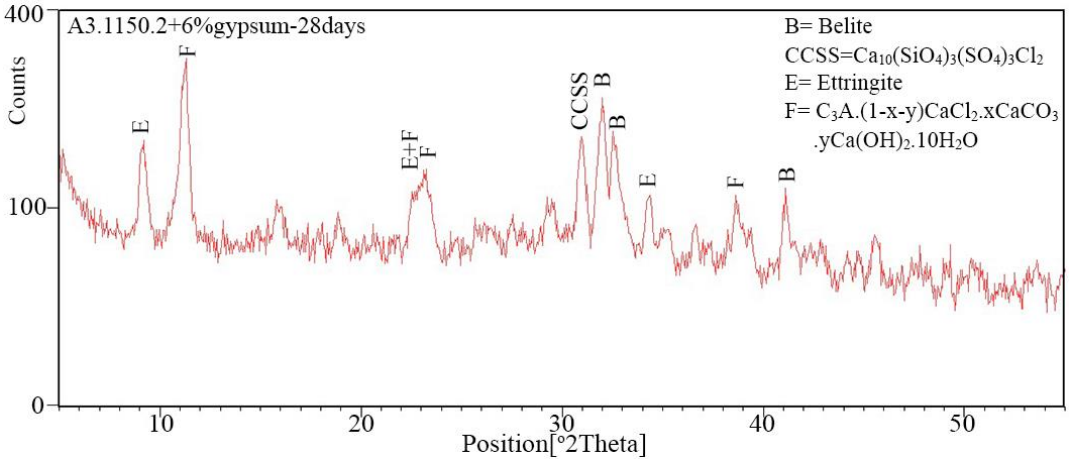

Figure 16: XRD Pattern of paste of A3.1150.2+6% at 28 days.

A3.1150.2+6% paste – 28 days
Belite [C_2S]
Calcium Chloride Silicate Sulfate [$Ca_{10}(SiO_4)_3(SO_4)_3Cl_2$]
Ettringite [$C_3A.(CaSO_4)_3.32H_2O$]
Friedel's salt [$C_3A.(1\text{-}x\text{-}y)CaCl_2.xCaCO_3.yCa(OH)_2.10H_2O$]

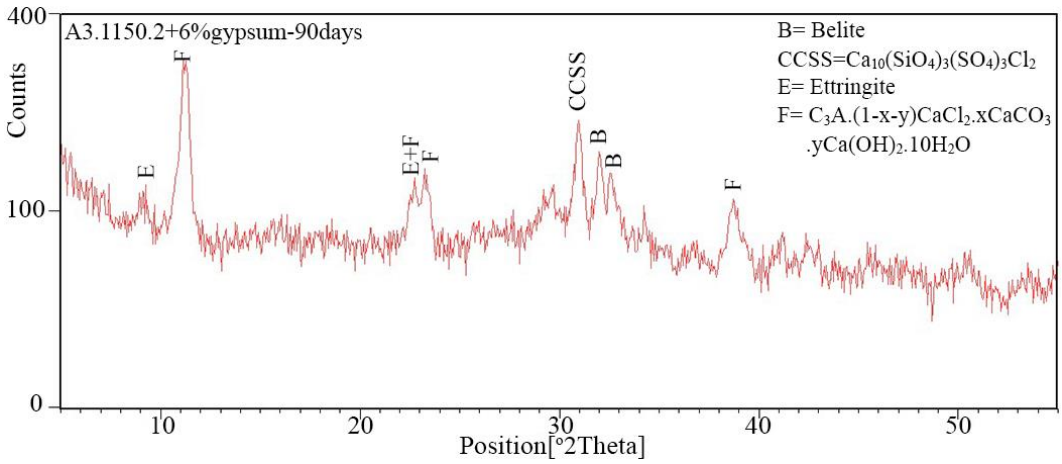

Figure 17: XRD Pattern of paste of A3.1150.2+6% at 90 days.

A3.1150.2+6% paste – 90 days
Belite [C_2S]
Calcium Chloride Silicate Sulfate [$Ca_{10}(SiO_4)_3(SO_4)_3Cl_2$]
Ettringite [$C_3A.(CaSO_4)_3.32H_2O$]
Friedel's salt [$C_3A.(1\text{-}x\text{-}y)CaCl_2.xCaCO_3.yCa(OH)_2.10H_2O$]

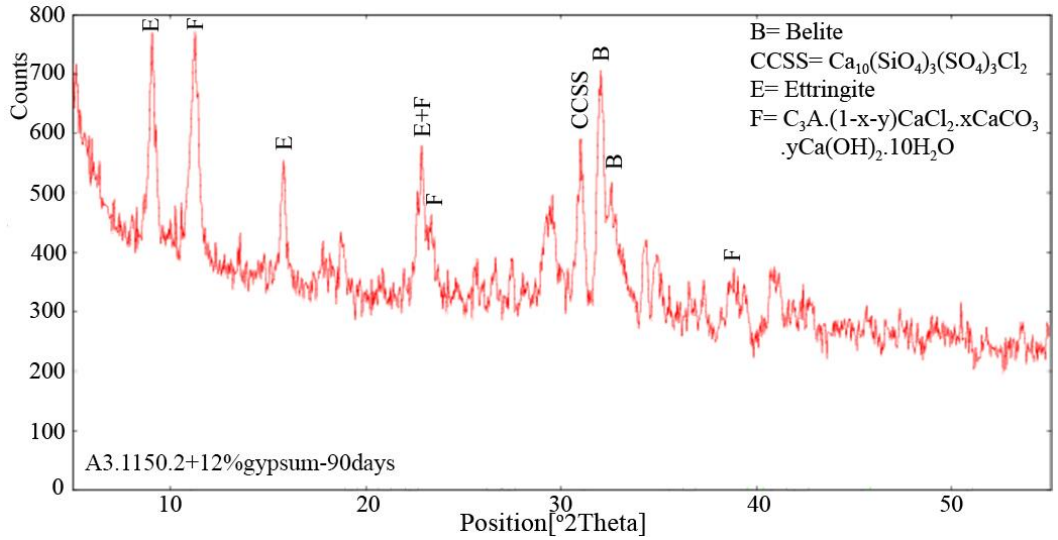

Figure 18: XRD Pattern of paste of A3.1150.2+12% at 90 days.

A3.1150.2+12% paste – 90 days
Belite [C_2S]
Calcium Chloride Silicate Sulfate [$Ca_{10}(SiO_4)_3(SO_4)_3Cl_2$]
Ettringite [$C_3A.(CaSO_4)_3.32H_2O$]
Friedel's salt [$C_3A.(1\text{-}x\text{-}y)CaCl_2.xCaCO_3.yCa(OH)_2.10H_2O$]

Alinite phase seems to reduce after 2 days, an indication of its fast hydration. Belite, however, is present up to 28 days, and its peaks are still noticeable even at 90 days. This is considered to be the main reason behind the significant strength difference between 28 days and 90 days strength of A3 samples. Belite being a slow reacting compound, becomes effective in the late strength of alinite cement.

Ettringite is also observed and although its intensity decreases at 90 days, it is observable between 6 hours and 90days. Ettringite peaks are notably more intense in the case of 12% gypsum addition, as expected.

Unlike A2 samples, peaks of calcium hydroxide are not apparent in A3 diffractograms. One obvious reason for that is the fact that hydration rate of A2 is higher than A3, as can be seen from compressive strength results. Another reason is that alinite/belite ratio is lower in A3 clinker relative to A2 clinker, as indicated by clinker diffractograms. Therefore, less calcium hydroxide comes out in the case of A3 hydration for the same amount of C-S-H formation. Another possible explanation is the possibility of leaching of calcium hydroxide into curing water. Since cure water was tap water, calcium hydroxide might have leached out through diffusion, as slow strength gain leaves relatively large capillary pores continuous for a longer time. XRD diffractogram of a sample taken from the top of cure water of A3 samples confirms this argument.

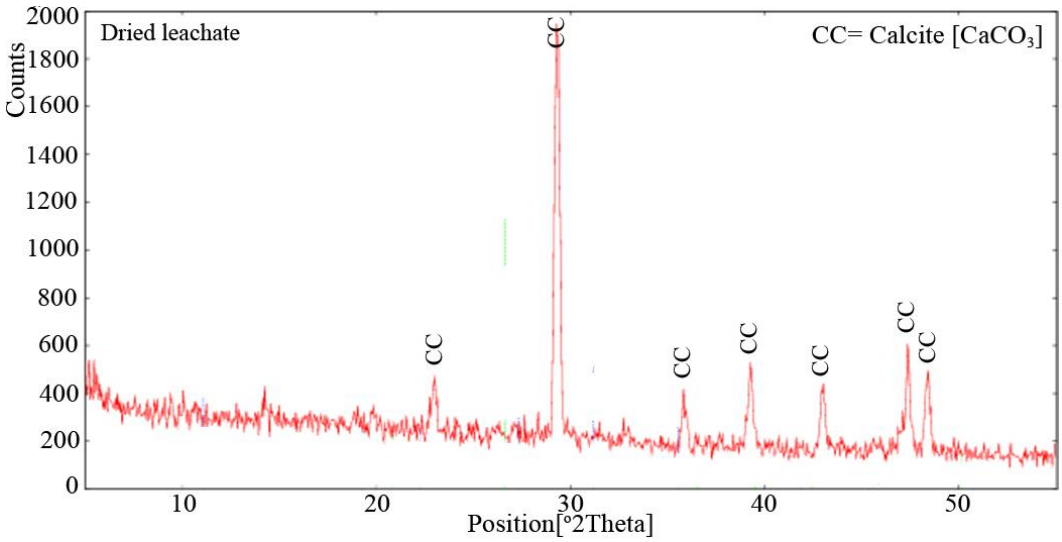

Figure 19: XRD Pattern of dried leachate.

Finally, rest is turned into calcium carbonate, which is the reason of the peaks on 29^{o} in diffractograms.

4.3.5 Scanning Electron Microscopy

Scanning electron microscope images were taken to visually observe the hydration products. Results of some A3 samples at various ages are presented below. Images of A2 samples and additional A3 samples are provided in Appendix B.

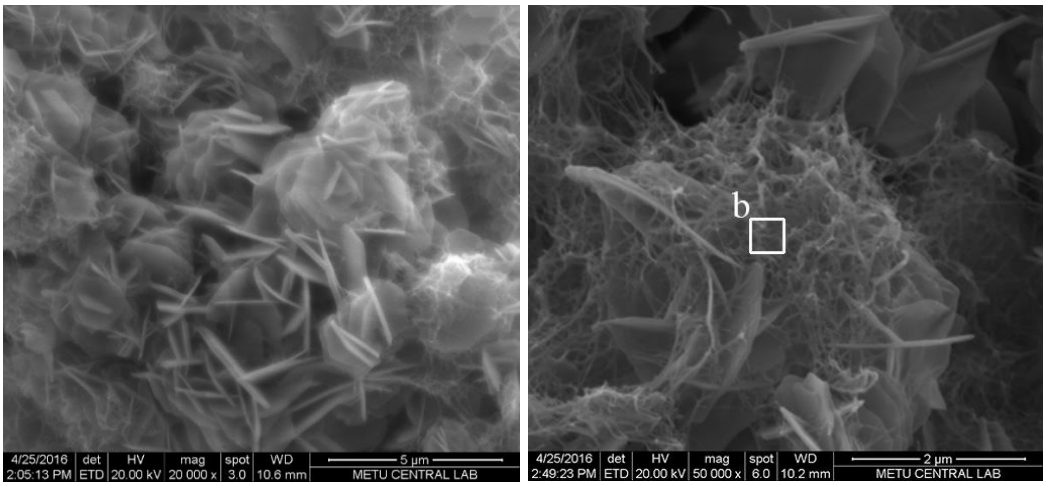

(A) (B)

Figure 20: SEM Images of hydrated A3.1150.2+6% (A) and A3.1150.2+12% (B) pastes at 2 hours of hydration.

In A3.1150.2 pastes (Fig. 20), two different hydration products were observed, starting from 2 hours. First one was the C-S-H gel, which has a reticular form at early hydration stages. The other was reported to be $C_3A(1-x-y)CaCl_2.xCa(OH)_2.yCaCO_3$, a phase similar to Friedel's salt, caused by the hydration of calcium aluminochloride. Presence of this phase is important as it is the main binder of chloride in the cementitious system.

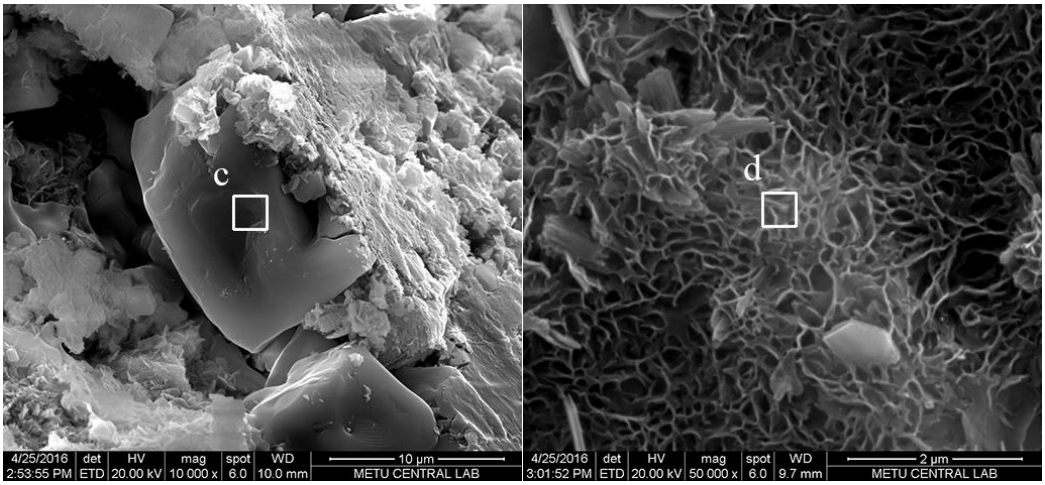

(C) (D)

Figure 21: SEM Images of hydrated A3.1150.2+6% paste at 6 hours (C) and 2 days (D) of hydration.

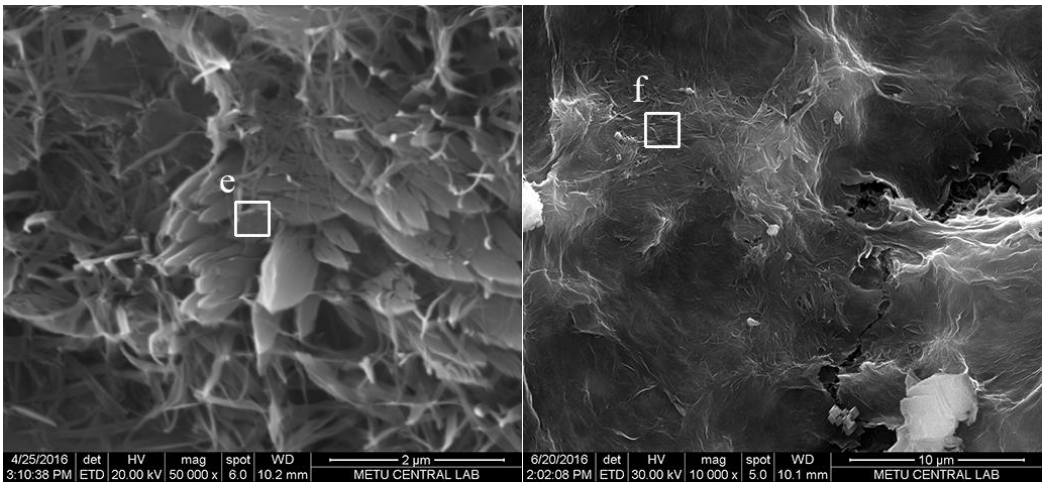

(E) (F)

Figure 22: SEM Images of hydrated A3.1150.2+6% paste at 28 days (E) and 90 days (F) of hydration.

At 6th hour of hydration, cubic shaped crystals started to appear (Figure 21 (C)). EDX analysis clearly showed that they were sodium chloride salt (see table 17). At

2nd day, C-S-H structure transformed into a honeycomb-like shape. In some parts, fibrous, more crystalline form of C-S-H was observed (Figure 22 (E)).

Intense layers of C-S-H were formed after 28 days. Calcium carbonates were precipitated on these layers. These carbonates are thought to be carbonated calcium hydroxides which appear during hydration reactions (visible in Figure 22 (F)).

Table 17: EDX Quantitative Analysis of Marked Points in Figure 20-22.

Element (wt %)	**b**	**c**	**d**	**e**	**f**
O	34.26	4.72	33.39	12.94	37.34
Ca	24.34	2.10	34.16	47.21	33.76
Si	7.43	0.50	13.21	5.42	8.63
Cl	7.33	49.89	0.30	3.71	7.71
C	10.38	7.79	9.71	9.42	-
Al	2.92	0.52	1.06	1.89	4.46
S	0.95	0.40	0.92	2.66	4.39
Mg	1.38	0.37	0.44	1.83	1.12
K	0.58	0.06	-	0.73	-
Na	1.65	26.64	0.11	0.47	-
Fe	1.49	0.34	0.78	2.77	2.60

CHAPTER 5

CONCLUSIONS AND FUTURE RECOMMENDATIONS

5.1 Conclusions

In this study, synthesis and optimization of the properties of alinite cement by using soda waste sludge as a raw material was investigated. It was concluded that:

1. Low-energy and low-CO_2 alinite cement clinker was successfully synthesized using soda waste sludge as partial replacement of limestone. Although it was also produced in 1050^oC, clinkers produced at 1150^oC yielded better results in terms of Cl, alkalis, and free CaO content.
2. Clinkerization failed in the case of soda waste sludge as the only calcium source. This was attributed to soda waste sludge's low calcium and high chlorine content in its unprocessed form.
3. Compressive strength did not change significantly between 1, 2, and 4 hours of calcination time. Yet, chemical compositions were slightly improved as calcination time increased. As a result, 2 hours of calcination time were found suitable.
4. Alinite cement clinker was less dense than portland cement clinker. A2 clinker had a density of 3.03 g/cm^3 and A3 clinker had a density of 3.00 g/cm^3 while portland cement clinker had a density of 3.26 g/cm^3.
5. Alinite cement clinker was significantly easier to grind. 60 minutes of grinding was required to obtain 3500 cm^2/g specific surface area in the case of A3.1150.2 clinker. Portland cement clinker required 195 minutes of grinding to reach the same specific surface area value.

6. Normal consistency tests showed that alinite cement required less water than portland cement for the same consistency. This enabled usage of less water for compressive strength tests without reduced workability.
7. Regardless of mix and gypsum content, setting time of alinite cement was very rapid relative to portland cement. Gypsum content of A3 samples did not affect setting time significantly. This property of alinite cement might be advantageous in repair applications.
8. Calorimeter tests revealed that induction period, which is typical in portland cement hydration, did not occur during alinite cement hydration. Increasing gypsum content increased heat flow peaks of A3 samples, but total heat generation did not change significantly.
9. A2.1150.2+6% sample, which had 2 days compressive strength value comparable to portland cement sample, generated twice as much heat compared to portland cement within this period. Total heat generation of A3.1150.2+6% sample, which had half the compressive strength value of portland cement sample at 2 days, was close to portland cement sample in first 2 days. So, it can be inferred that alinite cement in this study generates twice as much heat relative to portland cement to impart similar compressive strength values in first 2 days of hydration.
10. Alinite, belite, and calcium aluminochloride phases were observed in clinker XRD diffractograms. Ettringite and Friedel's salt-like phase were appeared upon hydration of A3.1150.2+6%. Belite peaks were still notable at 28 days. This explains the compressive strength difference of A3 samples between 28 days and 90 days.

    Portlandite peaks were also observed in hydrated A2.1150.2+6%. This confirms the occurrence of hydration reaction which forms C-S-H gel along with calcium hydroxide.
11. SEM results showed that C-S-H gel and hexagonal crystals of Friedel's salt-like phase are the main hydration products. Calcium carbonates and sodium chloride were also detected.

5.2 Recommendations for future studies

Soda waste sludge used in this study was in unprocessed form. In this state, chlorine content of the waste is very high. This permitted the use of waste only as partial replacement of limestone. Normally, this sludge is filtrated before disposal to get rid of excess chlorine. This filtrated form of the waste could be used to utilize soda waste as the only calcium source in production of alinite cement.

One major drawback of alinite cement production is its detrimental effect on metal production equipment. When exposed to exit gas, metal parts of the furnace, including heater resistances, started to corrode. Therefore, it is recommended that a furnace in which heaters are not directly exposed to exit gas should be used for alinite cement clinker production. It was noted that exit gas tube, which was made of mullite, was unharmed. So, it can be considered as the cover material of production chamber.

Exit gas of calcination process should be examined in order to identify the composition of the gas and to assess whether the gas composition is harmful or not.

This study investigated production and hydration properties of alinite cement. Yet, durability characteristics of alinite cement mortar and alinite cement concrete require further investigation. Water soluble chlorine content and effects of sodium chloride salt which appeared in SEM images should be determined. Durability against corrosion and physical salt attack should be checked.

Alinite cement’s interaction with portland cement and supplementary cementitious materials could also be investigated.

REFERENCES

ASTM C188-15. (2015). *Standard Test Method for Density of Hydraulic Cement*. ASTM International, West Conshohocken, PA.

ASTM C1437-15. (2015). *Standard Test Method for Flow of Hydraulic Cement Mortar*, ASTM International, West Conshohocken, PA.

Boikova, A.T., Grishchenko, L.V., and Domansky, A. I. (1986). Hydration activity of chlorine containing phases. In *Proceedings 8th ICCC* (pp. 275–276). Rio de Janeiro.

C.A. Hendriks, E Worrell, D. De Jager, K. Blok, & P. Riemer. (2002). Emission Reduction of Greenhouse Gases from the Cement Industry. *World*, 1–11.

Duda, Walter H. (1985). *Cement Data Book*, Vol.1, Bauverlag, Wiesbaden Berlin, 3rd Ed..

EN 196-1. (2009). *Methods of Testing Cement - Part 1: Determination of Strength*.

EN 196-2. (2010). *Methods of Testing Cement- Part 2: Chemical Analysis of Cement*.

EN 196-3:2005+A1:2008. (2008). Methods of Testing Cement - Part 3: Determination of setting time and soundness.

EN 196-6. (2010). *Methods of Testing Cement - Part 6: Determination of Fineness*.

Ftikos, C., & Kiatos, D. (1994). The effect of chlorides on the formation of belite and alinite phase. *Cement and Concrete Research*, *24*(1), 49–54.

Ftikos, C., Philippou, T., & Marinos, J. (1993). A study of the effect of some

factors influencing Alinite clinker formation. *Cement and Concrete Research*, *23*(6), 1268–1272.

Gao, C., Dong, Y., Zhang, H., & Zhang, J. (2007). Utilization of distiller waste and residual mother liquor to prepare precipitated calcium carbonate. *Journal of Cleaner Production*, *15*(15), 1419–1425.

Hendrik G. van Oss. (2015). Cement - Mineral Commodity Summaries. *U.S. Geological Survey*, (703), 38–39.

IPCC. (2007). IPCC Fourth Assessment Report (AR4). *IPCC*, *1*, 976.

Ji, L., Ren, X., and Su, H. (1997). Effect of chloride on hydration properties of alinite cement. In *Proceedings 10th ICCC* (p. 2ii030). Göteborg.

Juenger, M. C. G., Monteiro, P. J. M., Gartner, E. M., & Denbeaux, G. P. (2005). A soft X-ray microscope investigation into the effects of calcium chloride on tricalcium silicate hydration. *Cement and Concrete Research*, *35*(1), 19–25.

Kesim, A. G., Tokyay, M., Yaman, I. O., & Ozturk, A. (2013). Properties of alinite cement produced by using soda sludge. *Advances in Cement Research*, *25*(2),

Mowla, D., Jahanmiri, A., & Fallahi, H. R. (1999). Preparation and Optimization of Alinite Cement in Various Temperatures and CaCl2 Content. *Chemical Engineering Communications*, *171*(1), 1–13.

Neubauer, J., & Pöllmann, H. (1994). Alinite — Chemical composition, solid solution and hydration behaviour. *Cement and Concrete Research*, *24*(8), 1413–1422.

Noudelman, B., Bikbaou, M., Sventsitski, A., & Ilukhine, V. (1980). Structure and properties of a finite and alinite cements. In *7th International Congress on the Chemistry of Cement. Vol. 3* (p. V-169-174).

Noudelman, B. I., & Gadaev, A. I. (1986). Aspects Physico-Chimiques de la Cristallisation des Chlorsilicates lors de la Clinkerisation a basse Temperature

dans le bain fondu de sel. In *8th International Congress on the Chemistry of Cement. Vol. 2* (pp. 347–351).

Odler, I. (2000). *Special Inorganic Cements*, Modern Concrete Technology.

Pradip, Vaidyanathan, D., Kapur, P. C., & Singh, B. N. (1990). Production and properties of alinite cements from steel plant wastes. *Cement and Concrete Research*, *20*(1), 15–24.

Ruilun, Y., Bolin, W., Xinrong, W. (1984). In *Proceedings of the 8th International Congress on Chemistry of Cements* (pp. 122–127). Rio de Janerio.

Singh, M., Kapur, P. C., & Pradip. (2008). Preparation of alinite based cement from incinerator ash. *Waste Management*, *28*(8), 1310–1316.

Tokyay, M. (2016). *Cement and Concrete Mineral Admixtures*. CRC Press. Boca Raton.

U.S. Geological Survey 2016. (2016). *Mineral commodity summaries 2016*. *U.S. Geological Survey*.

APPENDICES

APPENDIX A

XRD PATTERNS OF CLINKERS

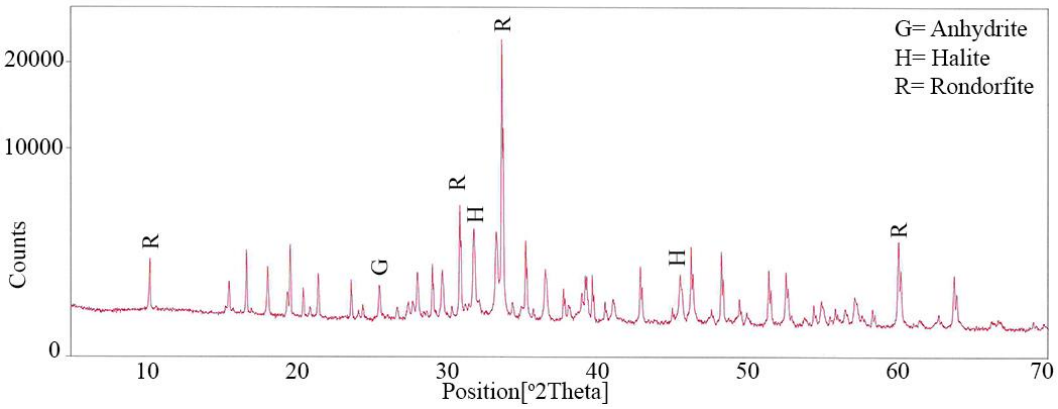

Figure 23: XRD Pattern of A1.1050.1.

A1.1050.1
Anhydrite [$CaSO_4$]
Halite [NaCl]
Rondorfite [$Ca_8Mg(SiO_4)_4Cl_2$

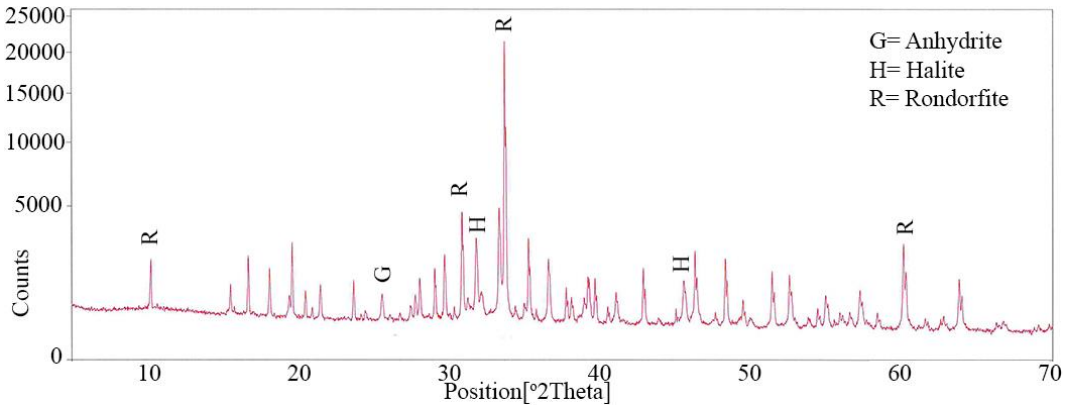

Figure 24: XRD Pattern of A1.1150.1.

A1.1150.1
Anhydrite [$CaSO_4$]
Halite [NaCl]
Rondorfite [$Ca_8Mg(SiO_4)_4Cl_2$]

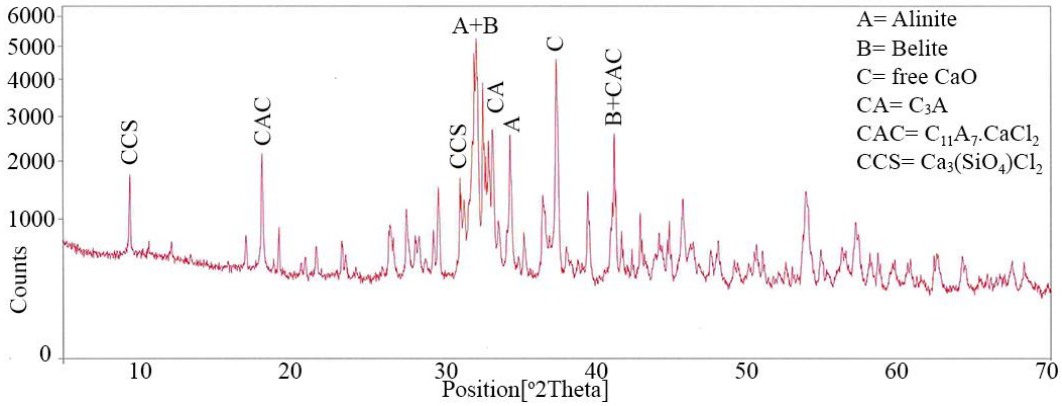

Figure 25: XRD Pattern of A2.1050.1.

A2.1050.1
Alinite [$Ca_{10}Mg_{0.8}[(SiO_4)_{3.4}(AlO_4)_{0.6}]O_2Cl$]
Belite [C_2S]
Free CaO
Aluminate [C_3A]
Calcium Aluminochloride [$C_{11}A_7CaCl_2$]
Calcium Chloride Silicate [$Ca_3(SiO_4)Cl_2$]

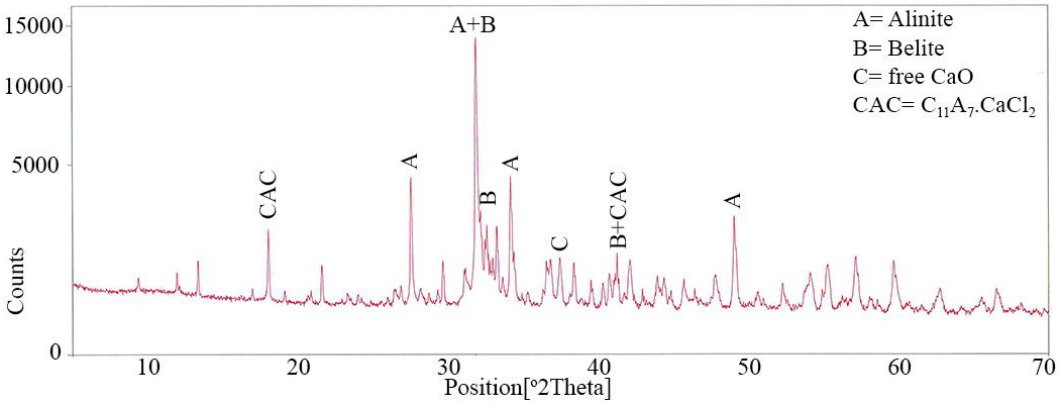

Figure 26: XRD Pattern of A2.1150.1.

A2.1150.1
Alinite [$Ca_{10}Mg_{0.8}[(SiO_4)_{3.4}(AlO_4)_{0.6}]O_2Cl$]
Belite [C_2S]
Free CaO
Calcium Aluminochloride [$C_{11}A_7CaCl_2$]

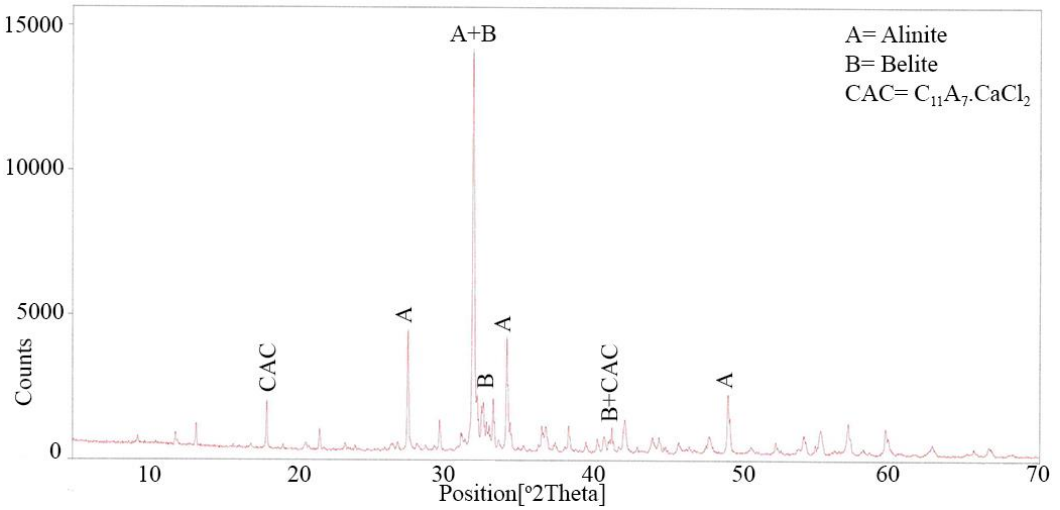

Figure 27: XRD Pattern of A2.1150.4.

A2.1150.4
Alinite [$Ca_{10}Mg_{0.8}[(SiO_4)_{3.4}(AlO_4)_{0.6}]O_2Cl$]
Belite [C_2S]
Calcium Aluminochloride [$C_{11}A_7CaCl_2$]

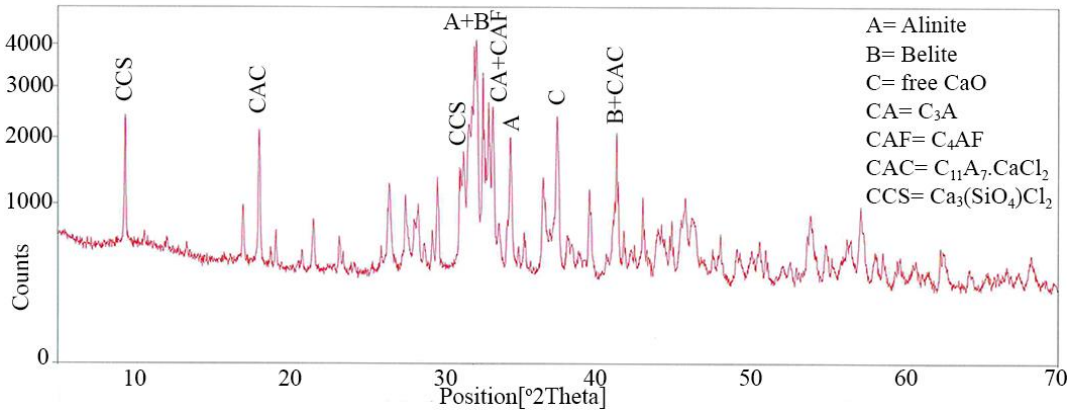

Figure 28: XRD Pattern of A3.1050.1.

A3.1050.1
Alinite [$Ca_{10}Mg_{0.8}[(SiO_4)_{3.4}(AlO_4)_{0.6}]O_2Cl$]
Belite [C_2S]
Free CaO
Aluminate [C_3A]
Ferrite [C_4AF]
Calcium Aluminochloride [$C_{11}A_7CaCl_2$]
Calcium Chloride Silicate [$Ca_3(SiO_4)Cl_2$]

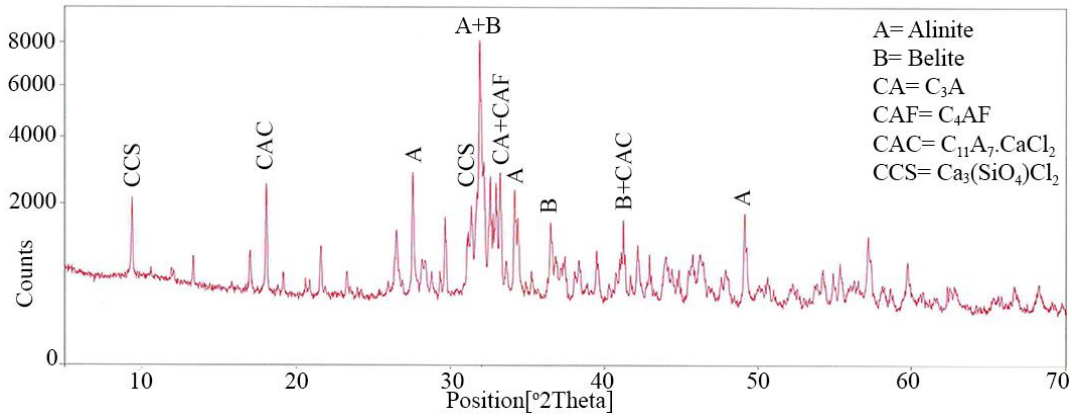

Figure 29: XRD pattern of A3.1150.1.

A3.1150.1
Alinite [$Ca_{10}Mg_{0.8}[(SiO_4)_{3.4}(AlO_4)_{0.6}]O_2Cl$]
Belite [C_2S]
Aluminate [C_3A]
Ferrite [C_4AF]
Calcium Aluminochloride [$C_{11}A_7CaCl_2$]
Calcium Chloride Silicate [$Ca_3(SiO_4)Cl_2$]

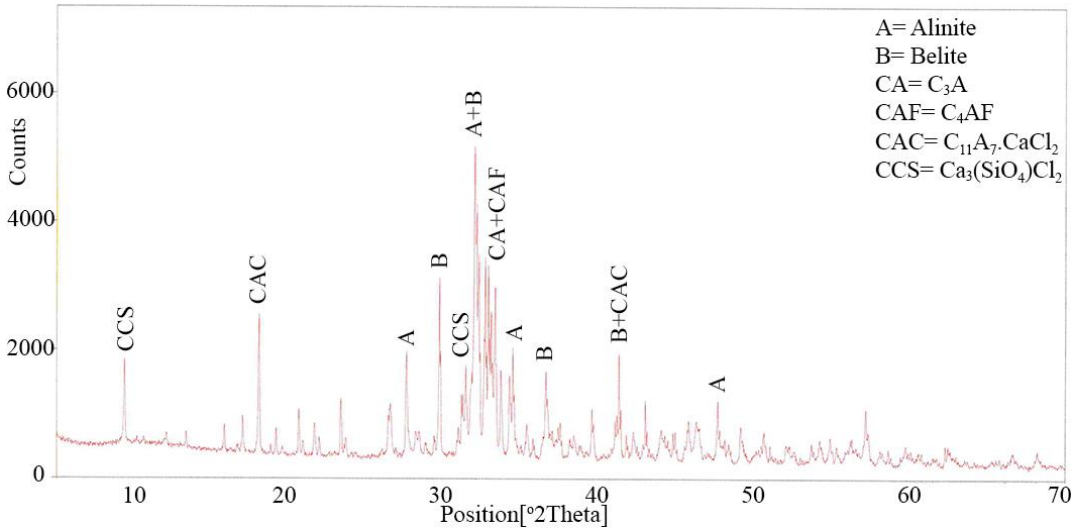

Figure 30: XRD pattern of A3.1150.4.

A3.1150.4
Alinite [$Ca_{10}Mg_{0.8}[(SiO_4)_{3.4}(AlO_4)_{0.6}]O_2Cl$]
Belite [C_2S]
Aluminate [C_3A]
Ferrite [C_4AF]
Calcium Aluminochloride [$C_{11}A_7CaCl_2$]
Calcium Chloride Silicate [$Ca_3(SiO_4)Cl_2$]

APPENDIX B

SEM IMAGES OF PASTES

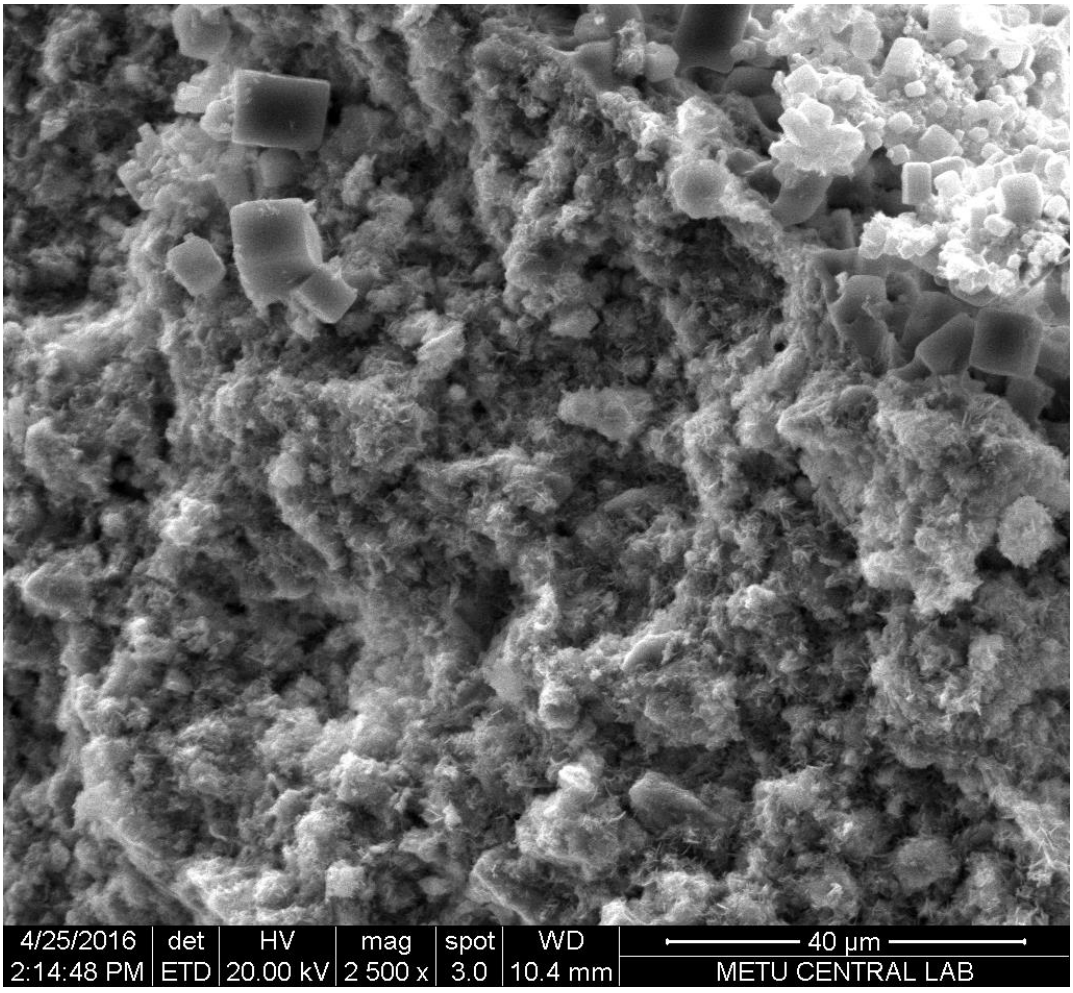

Figure 31: SEM image of A3.1150.2+6% paste at 6 hours of hydration.

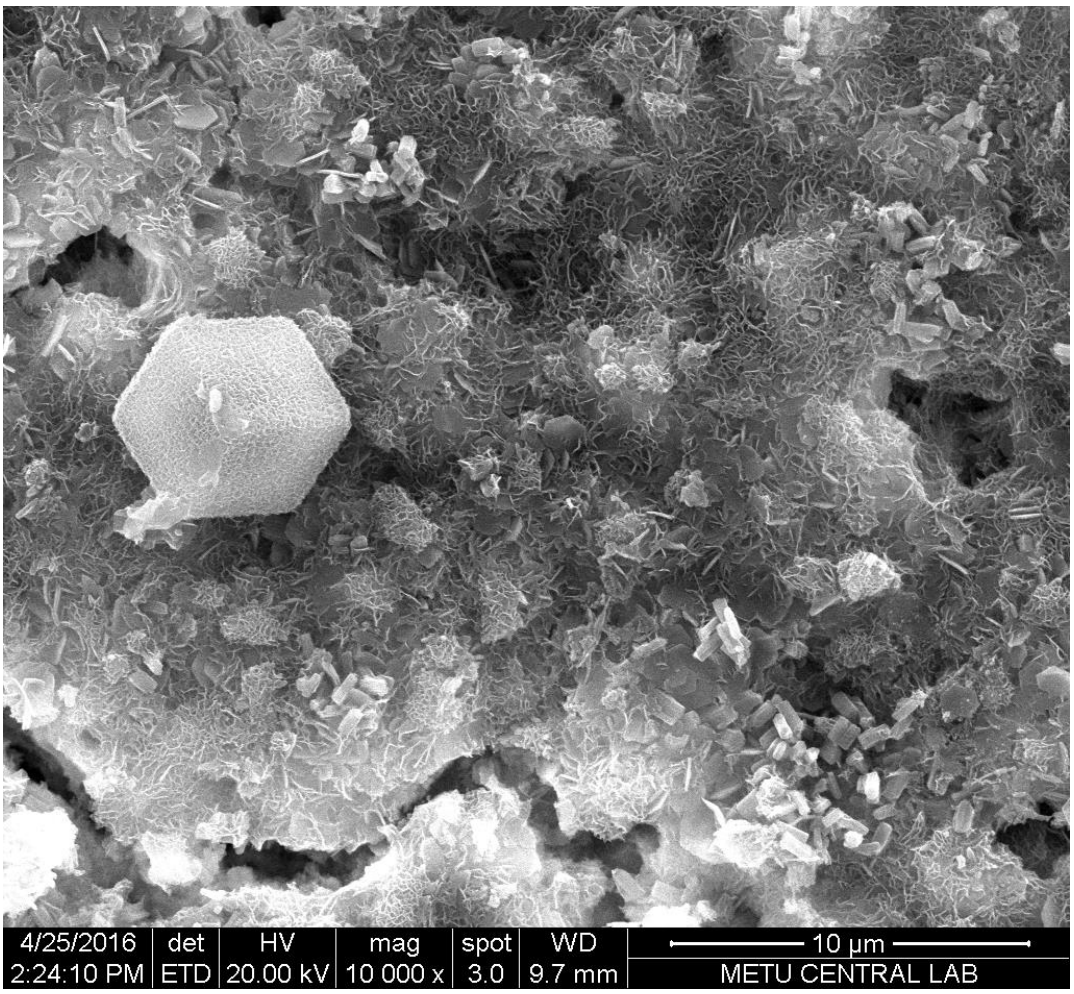

Figure 32: SEM image of A3.1150.2+6% paste at 2 days of hydration.

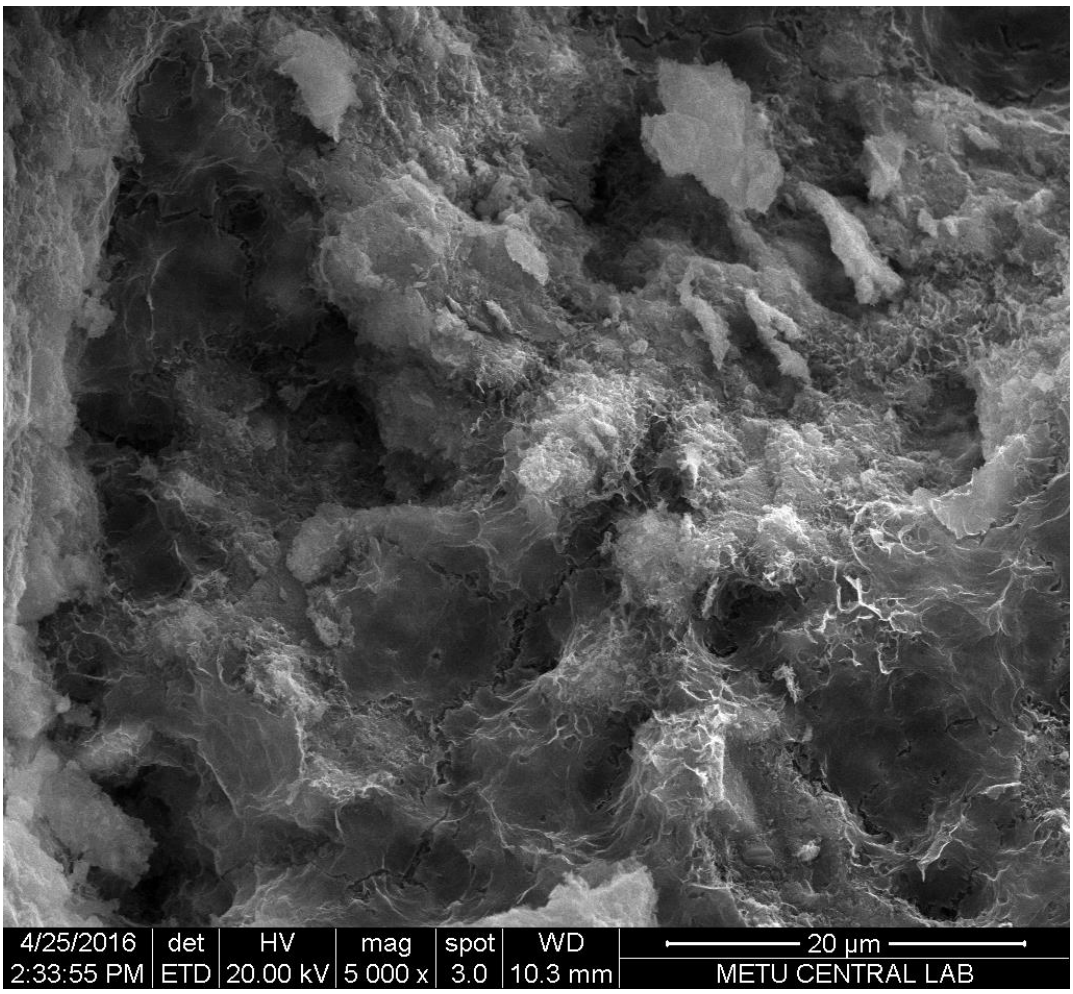

Figure 33: SEM image of A3.1150.2+6% paste at 28 days of hydration.

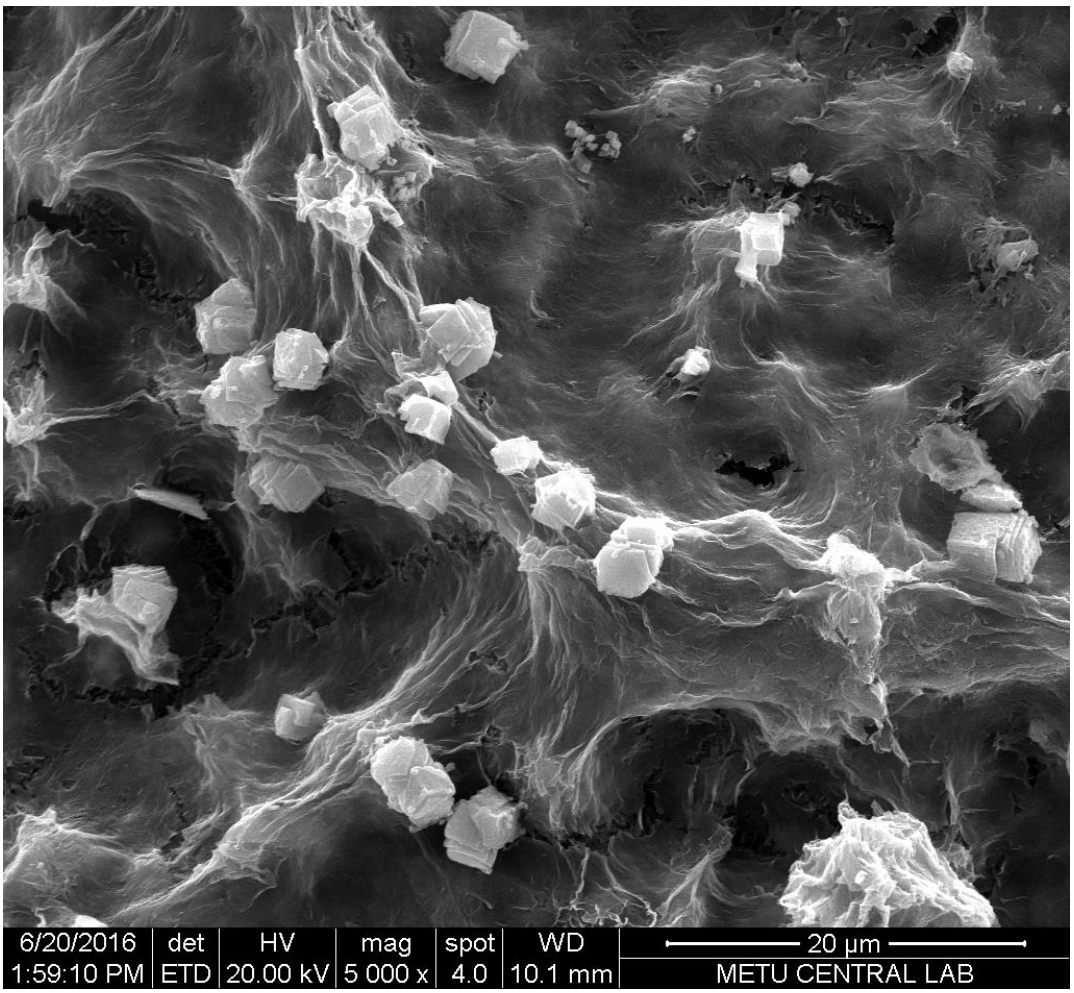

Figure 34: SEM image of A3.1150.2+6% paste at 90 days of hydration.

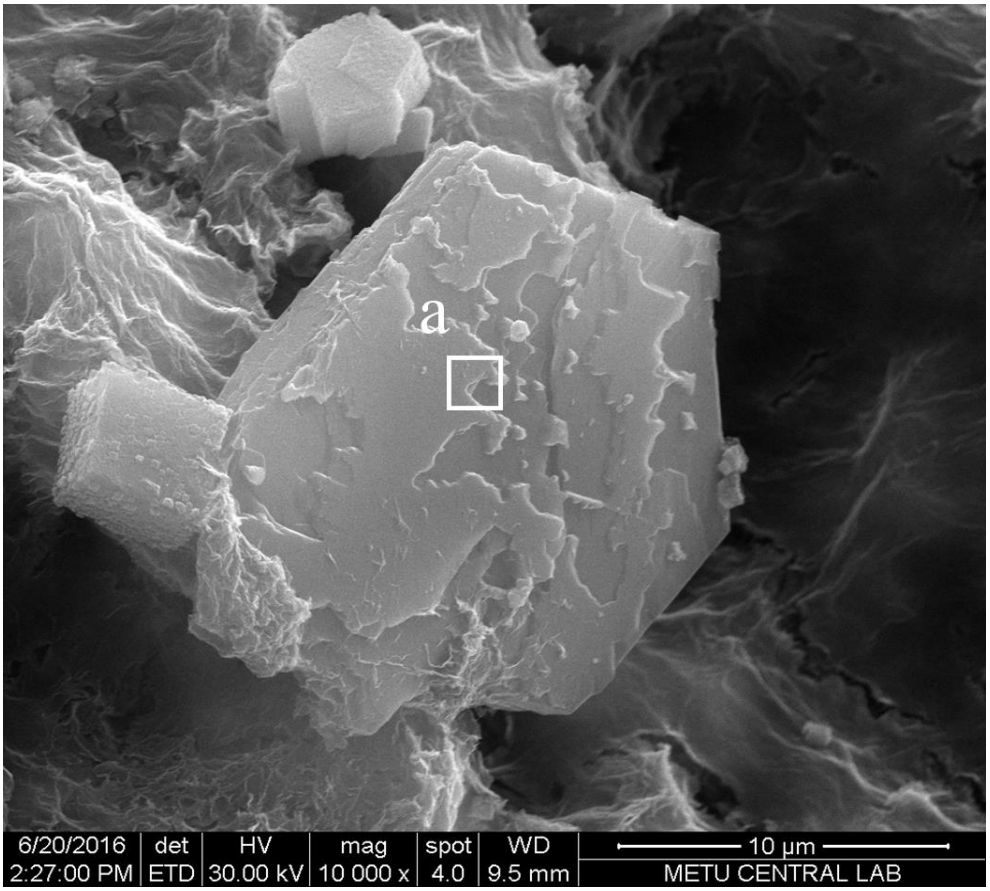

Figure 35: SEM image of Friedel's salt-like phase found in A3.1150.2+12% paste at 90 days of hydration.

Table 18: EDX Quantitative Analysis of point a in Figure 35.

Element (wt %)	**a**
O	46.75
Ca	20.38
Si	4.27
Cl	3.42
C	15.39
Al	7.33
S	0.70
Mg	1.09
Fe	0.67

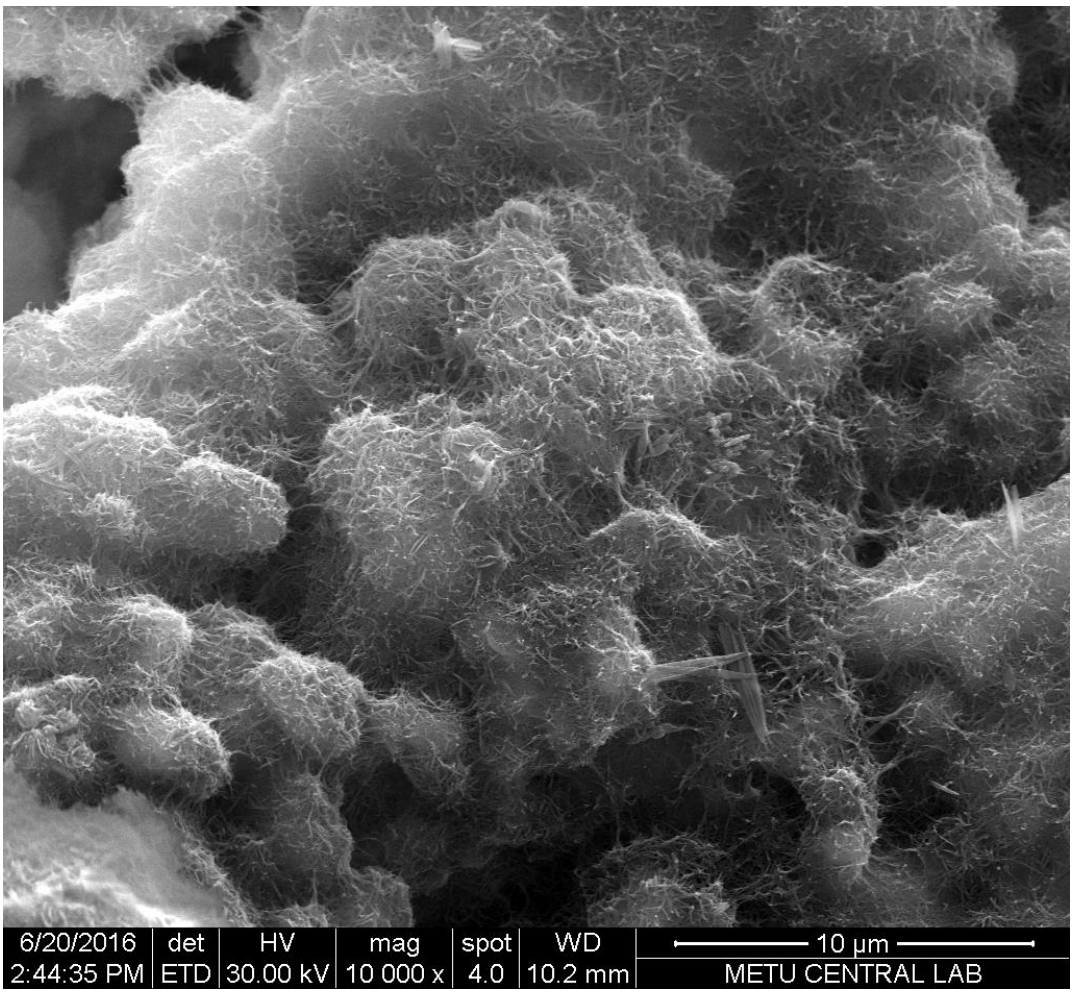

Figure 36: SEM image of A2.1150.2+6% paste at 6 hours of hydration.

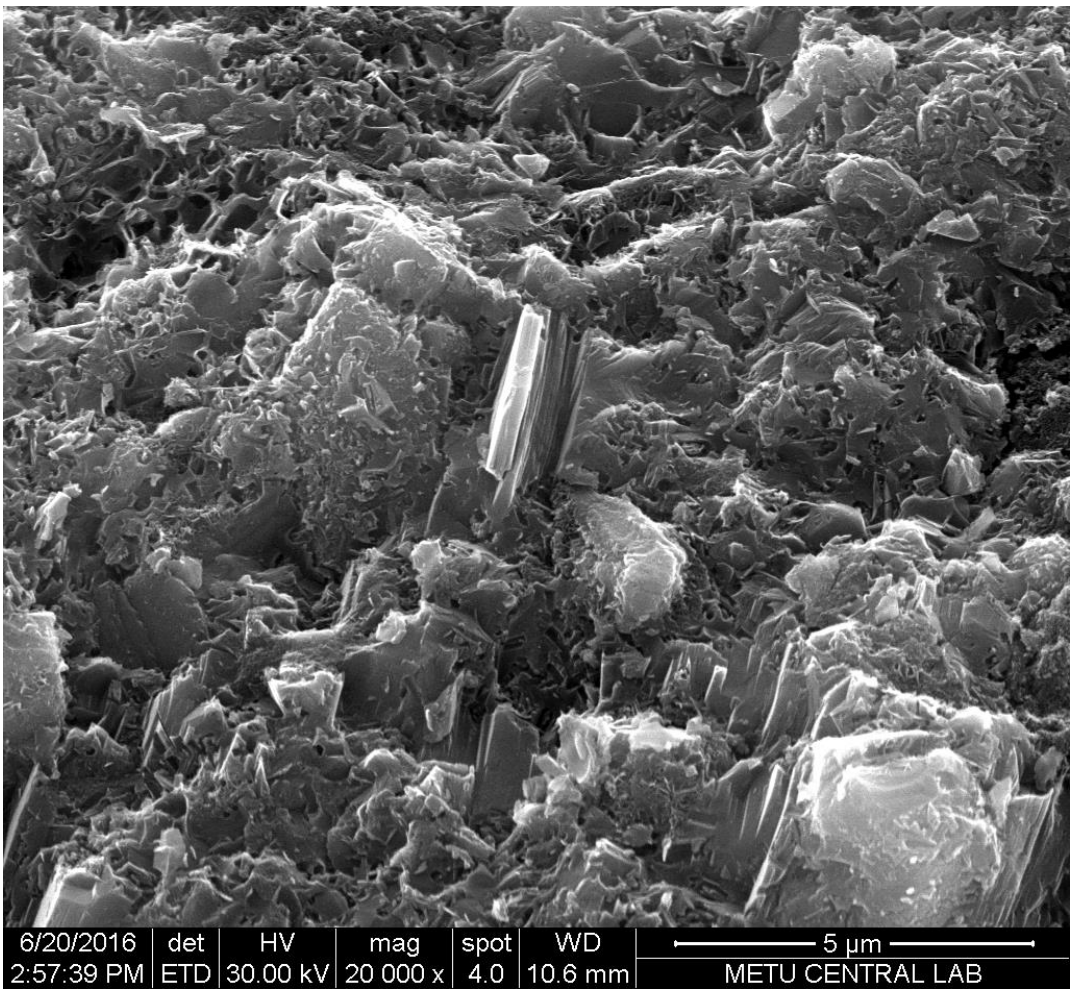

Figure 37: SEM image of A2.1150.2+6% paste at 28 days of hydration.